from BD Farmingen (San Diego, CA) or Beckman Coulter (Fullerton, CA), or Ancell Corporation (Bayport, MN). Aliquots of cell suspensions (4.5 x 10^4 cells) were mixed with primary antibody in a total volume of 90 μl and were incubated for 30 min at RT. The cell suspension was washed twice with PBS/FBS, and the cells were fixed in 200 μl of PBS/FBS containing 1% paraformaldehyde. Five thousand events were acquired for each antibody on a FACS Calibur apparatus using the CELLQuest acquisition software program (Becton, Dickinson and Company, Flanklin Lakes, NJ). *ZsGreen* expression was also examined in human ccdPAs. Non-transduced cells were used as a negative control.

Quantification of Transduced Gene

Genomic DNA was extracted from cultured cells and mouse adipose sections with the DNeasy Blood & Tissue kit and the Gentra Puregene kit (QIAGEN, Hilden, Germany), respectively. The integrated vector copy number was quantified with the SYBR *Premix Ex Taq* (Perfect Real Time) kit (TaKaRa Bio Inc.). A known amount of pCGThLCAT DNA was used as a standard. The primer pairs were from the Retrovirus Titer Set (TaKaRa Bio Inc.). The DNA content in a human normal cell (6 pg/cell) [22] was used for calculating the average integrated copy number. Existence of transduced gene in transplanted adipose tissue was quantified with a TaqMan Gene Expression Master Mix (Applied Biosystems, Foster City, CA) using *lcat*-cDNA specific primers and probes designed by the Probe Finder Software program (Roche Diagnostics, Mannheim, Germany). All the real-time PCR reactions were performed using the ABI7500 Real-time PCR system (Applied Biosystems).

Detection of LCAT Protein

Culture medium and mice sera were diluted to a volume of 500 μl with ice-cold phosphate buffered saline containing 0.2% Nonidet P-40 (PBS-NP40) and were incubated with 2.5 μl of anti-LCAT rabbit monoclonal antibody (EPITOMICS, Burlingame, CA) for 18 hrs at 4 °C with gentle rotation. Twenty micro-liters of TrueBlot anti-Rabbit Ig IP Beads (eBioscience, San Diego, CA) was added and incubated with rotation for 2 hrs at 4 °C. Bound proteins were pelleted by centrifugation, washed with PBS-NP40, and eluted by boiling in 10 μl of 2X Laemmli's sample buffer. Immunoprecipitated samples were subjected to immunoblotting. Purified human LCAT (Roar Biomedical, Inc., New York, NY) or human plasma HDL (Calbiochem, Merck, Darmstadt, Germany) was used as a standard. An anti-LCAT rabbit polyclonal antibody (Novus Biologicals, Littleton, CO) and TrueBlot anti-Rabbit IgG HRP (1:5000) (eBioscience) were used as primary and secondary antibodies, respectively. The signals were detected with the SuperSignal West Femto Maximum Sensitivity Substrate (Thermo Fisher Scientific Inc.) and the LAS1000 apparatus (FUJI film, Tokyo, Japan).

Measurement of LCAT Activity

The procedure described by Ishii *et al.* [23] was modified to prepare the liposome substrate for the LCAT analyses. Two hundred microliters of [^{3}H]-cholesterol (American Radiolabeled Chemicals, Inc., St. Louis, MO) were evaporated to dryness by flushing N_2 gas, and 5 ml of the substrate mixture of Anasolv LCAT kit (SEKISUI MEDICAL Co. Tokyo, Japan) was added. The solution was sonicated with a Digital Sonifier Model 250 (BRANSON, Danbury, CT) at an amplitude of 40% and 0.5 second pulse cycles for 1 min a total of six times in an ice bath. The sonicated mixture was centrifuged at 3,000 rpm and stored at 4 °C until use. The reaction mixture contained 100 μl of labeled substrate, 4.5 mM β-mercaptoethanol, 36 μg of apolipoprotein A1 (Athens Research & Technology, Athens, GA), and 100 μl of culture medium in a total volume of 220 μl. The reaction was performed at 37 °C for 1 hr, and was terminated by the addition of 1.6 ml of chloroform/methanol (2:1). One hundred microliters of water was added, and the organic phase was obtained by centrifugation. Fifty microliters of the organic phase was spotted onto Whatman flexible thin layer chromatography (TLC) plates (Whatman plc, Kent, UK). Sample-spotted plates were developed with standards of cholesterol and cholesterol oleate in a glass tank using a solvent mixture of hexane/ethyl ether/acetic acid (146:50:4) by TLC. Developed TLC plates were air-dried and stained with iodine (Wako Pure Chemicals, Osaka, Japan). Cholesteryl ester spots were excised, and the radioactivity was determined by liquid scintillation spectrometry.

Adipogenic Differentiation Assay

Human ccdPA (3.5 x 10^4 cells) were seeded into BioCoat Collagen I 48-well Multiwell Plates (BD Biosciences) and grown to confluency over 3 days. Differentiation was induced with the PGM Bullet Kit (Lonza, Basel, Switzerland), and the cells were incubated for 2 weeks. The cells were fixed in 4% paraformaldehyde, washed twice with PBS, incubated with 60% isopropanol for 1 min, and stained with Oil Red O solution (Chemicon International, Inc. Temecula, CA) for 20 min. The accumulation of triglycerides was examined to confirm adipogenic differentiation using the Triglyceride E-test kit (Wako Pure Chemicals) according to the manufacturer's instructions. The protein content of the lysate was also determined with the Quick Start Bradford Dye Reagent (Bio-Rad Laboratories Inc.).

Clonality Analysis by Southern Blotting

Abnormal amplification of specific cell clones resulting from the integration of the retroviral vector genomic sequence was examined by Southern blotting according to the DIG (Digoxigenin) protocol (Roche Diagnostics). Genomic DNA extracted with the Gentra Pure Gene kit (QIAGEN) was digested with *Hin*dIII (Roche Diagnostics). Digested DNA (6 μg) was subjected to agarose gel electrophoresis, followed by capillary transfer to a positively-charged nylon membrane (Roche Diagnostics). Human *lcat* cDNA was used as a template to synthesize probes by the PCR DIG Probe Synthesis kit (Roche Diagnostics). Hybridization was performed at 50 °C overnight. The membrane was washed and reacted with Anti-digoxigenin-AP, Fab fragments (Roche Diagnostics). The signals were detected using CDP-Star with the LAS1000 apparatus (FUJI film). As positive control, 293 (European Collection of Cell Cultures) cells were transduced with a neomycin-resistant gene-containing version of the *lcat*-expressing retroviral vector, and typical single copy-integrated clones were selected.

Colony Formation Assay by Soft-Agar Containing Medium

Anchorage-independent colony formation was examined by the soft-agar assay using the CytoSelect 96-well Cell Transformation Assay kit (Cell Biolabs, Inc., San Diego, CA). Ten thousand gene-transduced human ccdPAs were seeded into 96-well plates in triplicates along with 100, 1000, or 10,000 HeLa cells (European Collection of Cell Cultures) as a positive control.

Monitoring Human LCAT Secretion in Mouse Model

Animal experiments were performed in the Central Institute for Experimental Animals (CIEA, Kanagawa, Japan) according to the Ethical Guidelines for Animal Experimentation from CIEA to examine the delivery of LCAT protein *in vivo*. To identify the transplanted cells, cells were stained using the PKH26 Red Fluorescent Cell Linker kit for General Cell Membrane Labeling (Sigma-Aldrich) one passage prior to transplantation. Expanded cells were harvested, washed with Ringer solution containing 0.5% human serum albumin (HSA, Benesis Corp. Osaka, Japan) four times, and re-suspended to a final cell concentration of 3×10^7 cells/ml. The cell suspension (50 μl) was injected into the adipose tissue between the shoulder-blades of NOD/Shi-*scid* IL-2Rγ^{null} (NOG) mice [24]. Buffer alone was injected as a control. All mice were bred in a vinyl-isolator and six animals were sacrificed to collect serum samples at each time point (Day 1, and at 1, 3, and 6 months). Six and three animals were used for the transplanted and control groups, respectively, for each time point. The transplanted region was taken using fluorescent microscopy on a SZX16 reflected fluorescence system (OLYMPUS corp. Tokyo, Japan), and sections were frozen at -80 °C until use.

Statistical Analysis

Data are presented as means ± S.D. Statistical comparison were made by Student's *t*-test or by ANOVA followed by the post hoc Dunnett or Tukey test using the SPSS software program. The integrated copy number, positive rate, and LCAT activity were analyzed to determine whether there was a linear correlation between these variables. For this analysis, we calculated a linear correlation coefficient (Pearson r value) and the corresponding P-value (two tailed) based on these assumptions. In all cases, P-values of less than 0.05 were considered to be statistically significant.

RESULTS

Preparation of Gene-Transduced Human ccdPAs

The optimization of cell-processing steps was carried out with fat tissues obtained from 16 healthy volunteers (C001-C016). Adipose tissue-derived proliferative cells were assessed for their suitability in ceiling culture, gene transduction, and cell expansion, using two culture media, DMEM/F12-HAM supplemented with 20% FBS (DMEM/FBS) and MesenPRO medium, respectively. The ceiling culture was performed in DMEM/FBS in comparison to MesenPRO medium. The cell yield of C012 after the ceiling culture from 1 g adipose tissue was $7.1 \times 10^5 \pm 1.0 \times 10^5$ and $2.1 \times 10^5 \pm 0.2 \times 10^5$ cells in DMEM/FBS and MesenPRO medium, respectively, showing that a higher cell yield was obtained in DMEM/FBS than in MesenPRO medium ($p<0.05$). The flow cytometric analyses showed that cells in DMEM/FBS tended to be homogeneous in shape and size, in comparison to those grown in MesenPRO medium (Fig. **1a**). The gene transduction of the cells after the ceiling culture was next assessed using the two medium types. The above cells which were frozen after ceiling culture (C010) in DMEM/FBS were recovered, incubated for 4 days, and seeded for gene transduction in MesenPRO medium or DMEM/FBS medium. After transduction with the *lcat*-expressing retroviral vector, the cells were passaged several times in the respective medium, and cell samples were subjected to copy number quantification 12 days after transduction. DMEM/FBS was more effective than MesenPRO medium for the gene transduction of human ccdPAs when a retroviral vector was employed under the appropriate conditions (0.94 ± 0.10 copies/cell vs. 0.36 ± 0.09 copies/cell, $p<0.05$). Finally, the effects of the

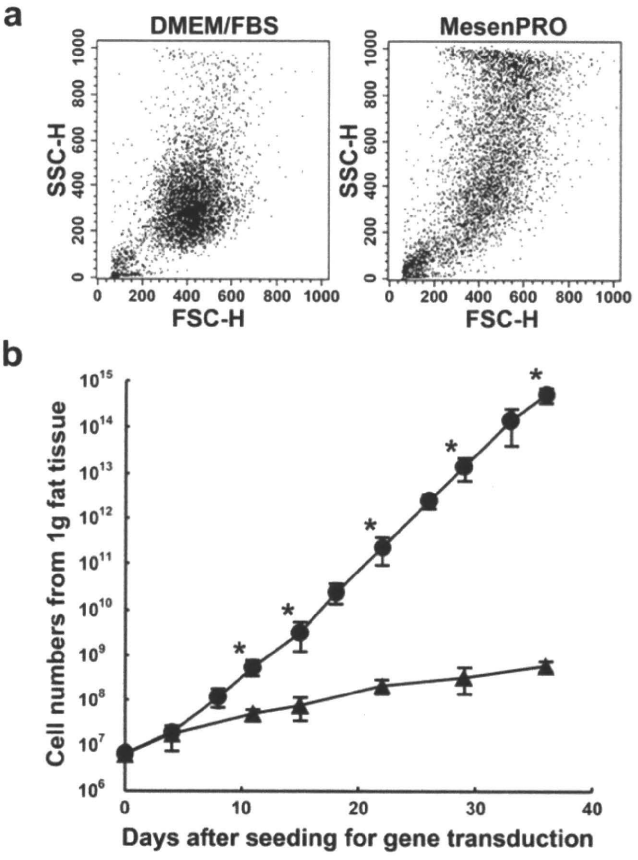

Fig. (1). Comparison of DMEM/FBS and MesenPRO media for the preparation of human ccdPAs. (**a**) The cells (C012) prepared by ceiling culture in DMEM/FBS (left panel) or MesenPRO medium (right panel) were subjected to a FACS analysis. The dot-plot (forward-scattered vs. side-scattered) of both cell populations are shown. A representative plot is shown for each medium. (**b**) The cells derived from C013 were used for expansion. Cell numbers were counted during proliferation for 35 days in DMEM/FBS (closed triangle) or MesenPRO medium (closed circle) after gene transduction in DMEM/FBS. Cell numbers are presented from 1 g of fat tissue. Data are presented as the mean ± SD (n=3). *$p<0.05$ vs. MesenPRO medium at each day after seeding.

incubation media on the gene-transduced cell expansion were examined in C013 cells. The doubling times of the cells in the MesenPRO medium were significantly shorter than those in DMEM/FBS (31.7 ± 4.8 hours vs. 119.4 ± 29.6 hours, $p<0.05$). The transduced cell number expanded to more than 3 x 10^4 fold of the original number in a month when grown in MesenPRO medium (Fig. **1b**). Therefore, DMEM/FBS was chosen for the ceiling culture and gene transduction, and the MesenPRO medium for cell expansion of ccdPA, respectively, in subsequent experiments.

Characterization of Human ccdPAs

The cell surface antigen profile was analyzed by FACS for human ccdPAs (Fig. **2a**). The populations of $CD31^-/CD45^-$ cells were significantly increased in the ccdPA preparation, in comparison to SVF-derived cells (99.1 ± 0.3% vs. 95.6 ± 0.1%, $p<0.05$), indicating that ceiling culture technique excludes CD31-positive and/or CD45-positive cell populations in comparison with cells prepared from SVF. The ccdPAs were positive for CD9, CD10, CD13, CD29, CD44, CD59, CD90, CD105, CD146, and HLA-ABC, and

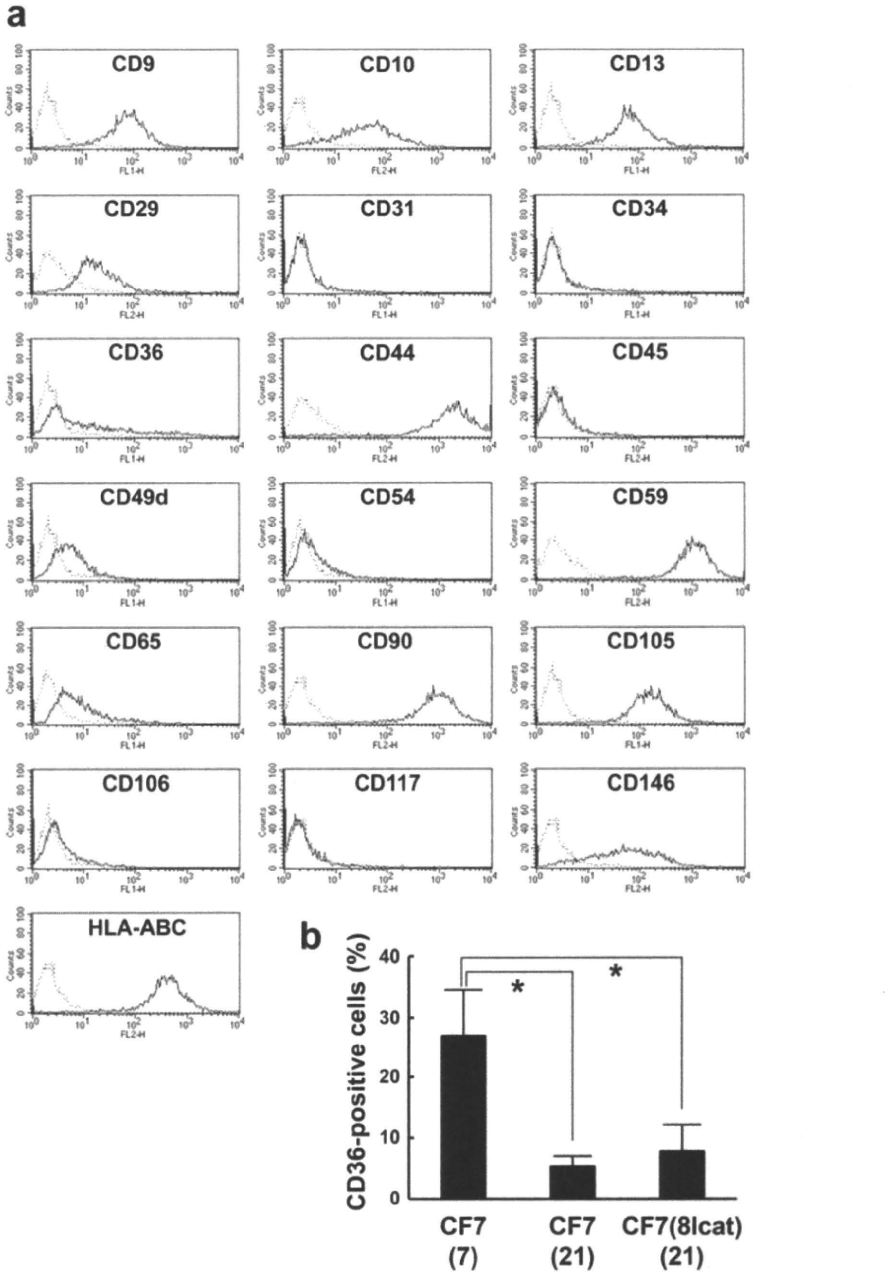

Fig. (2). Cell surface antigen profiles of isolated human ccdPAs by ceiling culture. (**a**) The cells were harvested at 7 days after ceiling culture, and were immuno-stained with the corresponding antibodies (solid line) or an isotype control (dotted line), and were subjected to a FACS analysis. Histograms for each antibody are presented. (**b**) CD36-positive cells was examined in the cells harvested from the ceiling culture (CF7(7)), the cells expanded after *lcat*-gene transduction (CF7(8lcat)(21)), and the cells expanded without gene transduction (CF7(21)). The ratio of CD36-positive cells in the prepared cells is presented as the positive cell rate (%). Data are presented as the mean ± SD (n=3). *$p<0.05$.

negative for CD31, CD34, CD45, CD54, and CD106. They were moderately positive for CD49d and CD65, and a substantial number of cells were positive for CD36, a marker for adipocytes [25]. The populations of CD36-positive cells after a 14-day *in vitro* culture of ccdPAs were significantly lower than those at 7 days ($p<0.05$, Fig. **2b**).

Retroviral Vector-Mediated Gene Transduction and Transduced Gene-Derived Protein Secretion in Human ccdPA

Human ccdPAs were evaluated as a recipient of MoMLV-based gene transduction using various concentrations of the vector and PS with single round of transduction using a ZsGreen-expressing vector. Two types of cells were analyzed, one cell type just after harvesting from the ceiling culture (CF7(7)), while another type was further cultured in the normal manner for an additional week (CF7(14)) in DMEM/FBS. The integrated copy number could be increased to approximately 1.7 and 2.5 copies/cell in CF7(7) and CF7(14) cells, respectively, and a good linear correlation was observed between the integrated copy number and the transduction efficiency (percentage of ZsGreen-positive cells) (Fig. **3a**). The transduction efficiency and the integrated copy number were significantly different between the cells of same batch at Days 1 and 2 of gene transduction (Fig. **3b**). These results showed that the cells with a higher transduction efficiency of the transduced gene and a lower integrated copy number were obtained by transduction for cells which were seeded and incubated overnight following a 7-day ceiling culture (CF7(8)). The CF7(8) cells were examined as a potential recipient for the human *lcat* gene. The transduction analyses using the *ZsGreen* vector showed that a vector concentration of 2.0×10^9 RNA copies/ml resulted in a good correlation between the integrated copy number and ZsGreen-positive cells in two different cell batches (Fig. **3a**). The use of the maximum achievable concentration (3.1×10^9 RNA copies/ml) of CGT_hLCATRV was compared with that using a concentration of 2.0×10^9 RNA copies/ml. Transduction of CF7(8) cells with 3.1×10^9 or 2.0×10^9 RNA copies/ml of the vector resulted in no difference in the integrated copy number (1.65 ± 0.12 vs. 1.56 ± 0.23 copies/cell). The LCAT protein produced by the *lcat* gene-

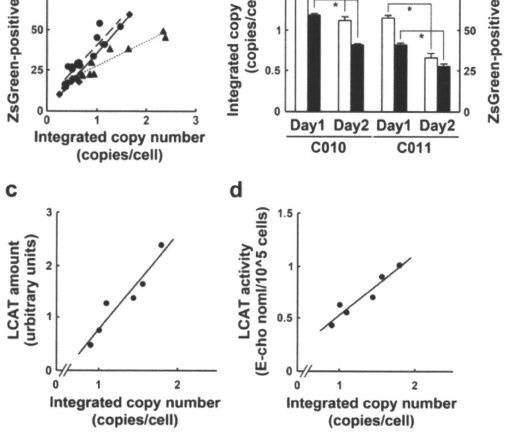

Fig. (3). ***In vitro*** **evaluation of human ccdPAs as recipients of MoMLV-based retroviral vector-mediated gene transduction and a vehicle for the secretion of functional LCAT protein.** (**a**) Integrated copy number (copies/cell) and ZsGreen-positive cells (%) were plotted for C010 CF7(7) (closed rhombus), C011 CF7(7) (closed circle), and C011 CF7(14) (closed triangle). Lines are drawn with Pearson r-values of 0.991, 0.908, and 0.937 for C010 CF7(7) (solid line), C011 CF7(7) (broken line), and C011 CF7(14) (dotted line), respectively ($p<0.05$). (**b**) Integrated copy numbers (copies/cell, open bars) and ZsGreen-positive cells (%, closed bars) after a single round of exposure of 2.0×10^9 RNA copies/ml of virus vector are shown. The cells (C010 and C011) were exposed to the transduction mixture one day (Day 1) or two days (Day 2) after seeding. Data are presented as the mean ± SD (n=3). *$p<0.05$. (**c**) Secreted LCAT protein was detected by immunoprecipitation/immunoblotting in culture medium incubated for 3 days with 1×10^5 cells (C013). After a densitometric analysis of immunodetected signals for human LCAT protein (60-65kDa), the integrated copy number and LCAT level (arbitrary units) were plotted (Pearson r-value of linear coefficient, 0.953, $p<0.05$). (**d**) Culture medium incubated with 1×10^5 cells (C013) for 3 days were subjected to assay of LCAT activities. The activity was presented by esterified cholesterol production from the cholesterol in the medium of human ccdPAs (Pearson r value of linear coefficient, 0.954, $p<0.05$).

transduced human ccdPAs was analyzed (Fig. **3c** and **3d**). Seven days after gene transduction, 1 x 10^5 cells were seeded in a 12-well plate, grown for three days, and the supernatant was collected for subsequent assays. LCAT protein production and the LCAT activity were determined by immunoprecipitation/immunoblot (IP-Western) and a cholesterol esterifying assay in the medium, respectively. LCAT protein and activity significantly correlated with the integrated copy number (r=0.917 and 0.954, respectively, p<0.05). Therefore, the activity of the LCAT protein produced by the gene-transduced ccdPA was estimated by the integrated copy number. The *lcat* gene-transduced ccdPAs produced LCAT protein with a specific activity of 5.2 ± 0.5 fmol esterified-cholesterol/integrated copy/hr in the culture medium within 3 days.

Properties of the *Lcat* Gene-Transduced Human ccdPAs during the Manipulation Process

The effect of *in vitro* manipulation was evaluated on the ccdPA characteristics regarding adipogenic differentiation ability, expansion rate, cell surface marker expression, transgene stability, and anchorage-independent cell growth. The cells were stimulated to differentiate and Oil Red O staining demonstrated the transduced cells had clearly differentiated into adipocytes (Fig. **4c**), and their appearance as well as that without differentiation stimulation, was not obviously different from cells without gene transduction (Fig. **4a-f**). The triglyceride contents showed no significant differences between transduced and control cells in C014 samples (1.30 ± 0.43 vs. 1.25 ± 0.27 mg/mg protein). The proliferating cell number and the resultant doubling time were not signifi-

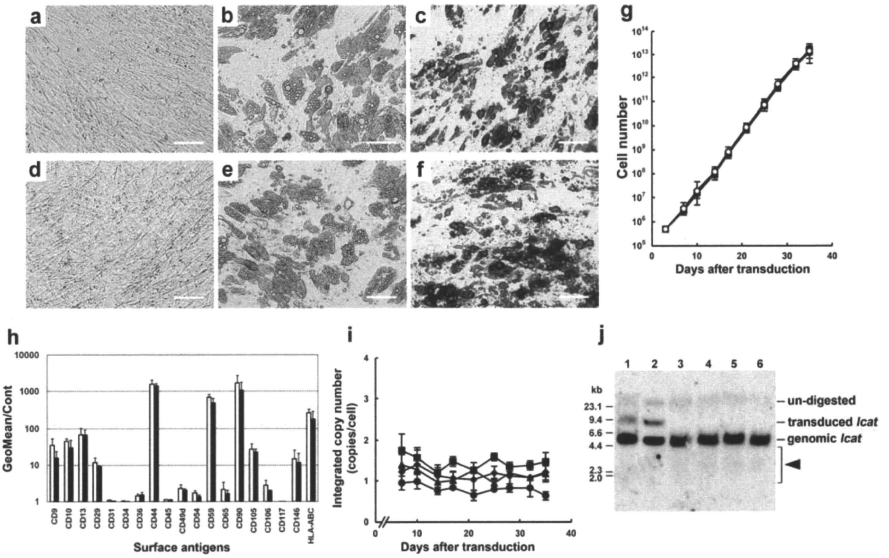

Fig. (4). Characterization of *lcat*-transduced ccdPA in culture. The *lcat*-transduced (**a**, **b**, **c**) and non-transduced (**d**, **e**, **f**) cells of C013 were incubated for two weeks with (**b**, **c**, **e**, **f**) or without (**a**, **d**) differentiation stimulation. The appearance of cells was observed with (**c**, **f**) or without (**a**, **b**, **d**, **e**) Oil Red O staining (magnification bar, 100 μm). (**g**) C013 cells were transduced, and the resultant cells were passaged. The cell numbers were counted during proliferation for 35 days. The cells were transduced by the conditions of 1.3 x 10^9 RNA copies/ml on Day 2 (closed circle), 1.3 x 10^9 RNA copies/ml on Day 1 (closed triangle), 2.0 x 10^9 RNA copies/ml on Day 1 (closed rhombus), or 3.1 x 10^9 RNA copies/ml on Day 1 (closed square). Doubling times were 32.2 ± 5.8 (closed circle), 31.5 ± 4.0 (closed triangle), 31.6 ± 3.9 (closed rhombus), and 31.3 ± 4.4 hrs (closed square), respectively. The doubling time of the control (non-transduced) cells (open circle) was 31.5 ± 4.7 hrs. Data are presented as the mean ± SD (n=3). No significant differences were observed in comparison to the control cells. (h) The *lcat*-transduced cells (closed bars) and non-transduced cells (open bars) were expanded in MesenPRO medium for two weeks after gene transduction. The values of Geo/mean for 19 different surface antigens were examined by a flow cytometry analysis. Data are presented as the mean ± SD (n=3). (**i**) The integrated copy number of *lcat*-transduced ccdPAs was followed during *in vitro* culture. Symbols are same as shown in Fig. **4G**. Data are presented as the mean ± SD (n=3). (**j**) A clonal analysis was performed by Southern blotting in C013 cells. C013 genomic DNA samples were prepared from the cells 18 days after gene transduction. Lanes 1 and 2, *lcat* gene-transduced clones obtained by transduction of 293 cells; lanes 3, 4, and 5, *lcat* gene-transduced human ccdPAs with different integrated copy number (lane 3; 0.90 ± 0.20; lane 4, 1.65 ± 0.12; and lane 5, 1.79 ± 0.23 copies/cell); lane 6, non-transduced (control) cells. A smeared faint signal was observed in the *lcat*-transduced ccdPAs (shown by arrow).

cantly different between the transduced cells and control cells (Fig. **4g**). In addition, no significant differences were observed in the cell surface marker expression levels between transduced and control cells (Fig. **4h**). The integrated copy number in the transduced ccdPAs was monitored to assess the fate of the transgene during the culture period for 35 days (Fig. **4i**). The integrated copy number did not significantly change after gene transduction. A Southern blot analysis using the human *lcat* gene as a probe revealed that only a faint signal was present independent of the genomic *lcat* locus, indicating that no amplification of a specific clone had occurred during the expansion process (Fig. **4j**). A soft agar assay showed that no anchorage-independent colony formation was present in the gene-transduced human ccdPAs (data not shown). These results demonstrated that the effect of gene transduction was negligible (or denied) on the characteristics of the obtained human ccdPAs regarding the differentiation, cell surface marker expression, transgene stability, and cell growth, in comparison to the non-transduced cells.

Circulating LCAT Supplementation by the Implantation of *Lcat* Gene-Transduced ccdPA in Mice

The capacity of human ccdPAs to be recipient cells for *lcat* gene product delivery was assessed in mice. A cell suspension containing 1.5 x 10^6 cells was transplanted into the fat tissue of immuno-deficient mice, and the levels of LCAT protein secreted into the serum was determined by the IP-Western method. Human LCAT was clearly detected in the sera of all transplanted mice at Day 1 (Fig. **5a**), and was detectable after a month in mice (Fig. **5b**). A densitometric analysis revealed that the concentration of human LCAT was approximately 0.26 ± 0.19 μg/ml at Day 1. The real-time PCR quantification of the adipose tissue transplanted with *lcat*-gene-transduced ccdPA showed that the *lcat* gene was present at 42.9 ± 27.1% (Day 1), 1.0 ± 1.0% (1 month), and 1.2 ± 0.7% (3 months) compared to transplanted cells at Day 0. These results suggested that approximately 1% of the *lcat* gene-transduced ccdPAs survived for 3 months after the transplantation of cells into the fat tissue of mice.

DISCUSSION

The current study evaluated autologous ccdPAs, the mature adipocye-derived cells, prepared from the subcutaneous fat of patients as a vehicle for therapeutic protein replacement therapy. Adipose tissue contains two major sources of proliferative cell populations, the floating (mature adipocytes) and pellet fractions (SVF), following the centrifugation of collagenase-digested fat tissue. This cell-based gene therapy was developed from the mature adipocyte cultures, since SVF consists of a heterogeneous cell population, including blood cells, fibroblasts, and endothelial cells [15, 16] and has some risks in yielding a cell population with an abnormal phenotype in long-term culture *in vitro* [26, 27]. The ceiling culture of the SVF-removed floating fraction can further enrich the cells derived (or dedifferentiated) from mature adipocytes by the buoyant property of adipocytes during the ceiling culture periods. Our ceiling culture excludes CD31- and CD45-positive cells, and our ccdPAs were negative for CD34, the marker for which adipose-derived stem cells are positive [28-30].

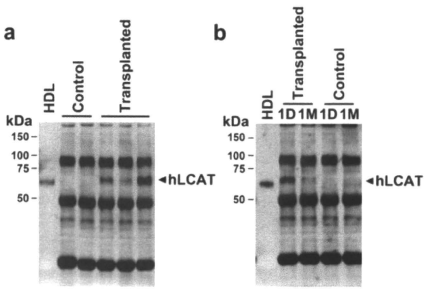

Fig. (5). Circulating human LCAT in NOG mice transplanted with *lcat*-transduced human ccdPAs. The cell suspension containing 1.5 x 10^6 *lcat*-expressing human ccdPA cells (C014, Transplanted) and Ringer's solution containing 0.5% HSA (Control) were injected into the fat tissue of NOG mice. After one day (**a**, **b**) or one month (**b**), the mice were sacrificed and serum samples were collected at each time point. D1, next day of injection; M1, 1 month after injection; H, 15 μg of HDL (control). At 1 month after transplantation, LCAT was detected in the serum of two mice out of six. At 3 months or later, LCAT was barely detectable in serum (data not shown).

MesenPRO medium, which is optimized for mesenchymal stem cells, provided some advantages in the preparation of ccdPAs through the higher expansion capacity in comparison to DMEM/FBS (Fig. **1b**). On the other hand, the MesenPRO medium was less effective for the propagation of human ccdPAs in ceiling culture than DMEM/FBS. Therefore, MesenPRO medium appears to be unsuitable for the proliferation of mature adipocytes in ceiling cultures. The FACS analyses showed that the obtained ccdPAs had a similar profile of surface markers with that of the previously reported adipose-derived cells [31, 32] (Fig. **2a**). In addition, the certain population of the ccdPAs retained a mature adipocyte marker (CD36) at an early stage and eventually lost it (Fig. **2b**). ccdPA exhibits clearly higher adipogenic potential in comparison to stromal vascular fraction derived cells, commonly used as multi-potential adipose tissue-derived stem cells, suggesting the advanced differentiation levels of ccdPA committed to mature adipocytes (manuscript in preparation). These adipogenic properties are sufficient for the cells to survive in fat tissue and to keep producing therapeutic protein for a long period after transplantation.

Previous reports described mature adipocyte-derived cells that were utilized and evaluated after primary culture for 2 weeks, and these cells were suggested to be a source of regenerative medicine [31, 32]. We demonstrated that 7-day primary cultures resulted in substantially better transduction properties than 14-day primary cultures for gene therapy applications. Simple exposure to the viral vector supernatant resulted in a 40-50% improved transduction efficiency (Fig. **3a** and **3b**) using 7-day culture ccdPAs, thus suggesting that human ccdPAs serve as an excellent recipient for retroviral vector-based therapeutic applications, in contrast to cell populations in which efficient transduction requires drug

selection [3, 33] or multiple rounds of transduction [34, 35]. Therefore, a single exposure to 2.0 x 10^9 RNA copies/ml of CGT_hLCATRV was selected to minimize the transgene copy number in each cell. Furthermore, the transduction efficiency was correlated with the integrated copy number (Fig. **3a** and **3b**). The *lcat*-expressing retroviral vector was constructed using pDON-AI, developed by Yu *et al.* [36], as a backbone vector. The risk of replication-competent retrovirus (RCR) occurrence was minimized by eliminating all the unnecessary structural genes from the MoMLV genome in this vector. In fact, no RCR was detected in the vector preparations (data not shown). The integration sites seemed to be randomly distributed since no clonal expansion was detected by a Southern blot analysis of the transgene following expansion culturing (Fig. **4j**), and no increase in the integrated copy number was observed in the preparations (Fig. **4i**). No evidence of transformation was observed in the soft agar assay, either at the time of implantation (after three weeks from fat tissue removal) or after long-term extended culture (data not shown). Furthermore, *in vivo* tumor formation assay by nude mice model revealed no abnormal cell growth after transplantation (unpublished observation). The safety issue of our therapeutic strategy will be carefully evaluated in future clinical studies.

The human *lcat* gene-transduced ccdPAs yielded the glycosylated LCAT protein (data not shown) that had a molecular weight and *in vitro* enzymatic activity equivalent to that observed in human serum. An animal study indicated that the human LCAT protein secreted from the implanted transduced human ccdPAs was detectable in blood samples (Fig. **5**). The serum of familial LCAT-deficient patients contains less than 10% LCAT activity compared to that in healthy subjects [11]. Patients with partially inactive LCAT enzymes (8.3-15% activity of the normal enzyme) have no renal complications [37-39]. Plasma infusion in patients, which raises the plasma LCAT activity level from 9.4% to 17.4% compared to normal subjects, resulted in a significant improvement of lipoprotein profiles [13]. These observations suggest that addition of approximately 10% wild-type LCAT enzyme into patients can prevent the development of the symptoms. The circulating LCAT protein concentration is approximately 6 μg/ml [11] in normal plasma. Transplantation of 1.5 x 10^6 of *lcat*-expressing human ccdPAs achieved nearly 5% of the healthy control level on Day 1 in mice (Fig. **5**), but LCAT delivery and cell survival were significantly decreased. Our recent experiments using an autologous mouse transplantation model showed a substantial improvement in LCAT delivery and cell survival (unpublished data), implying that 10^9 cells would yield a therapeutic effect in patients based on the weight ratio between mice and human (1:3000). The fact that the *lcat* gene-transduced human ccdPAs could be expanded to nearly 10^{10} cells within two weeks after gene transduction from 1 g of fat tissue suggested that human *lcat* gene-transduced ccdPAs may rescue LCAT deficient patients. Considering the differences in the lipoprotein metabolism between mice and humans, a future strategy to investigate the efficacy of human LCAT replacement therapy may be to establish an *in vitro* evaluation system employing serum obtained from familial LCAT-deficient patients.

In summary, the present study has established a procedure to prepare *lcat* gene-transduced human ccdPAs for clinical application. These cells have the ability to differentiate into mature adipocytes and secrete functional human LCAT protein. Animal studies revealed that the implanted cells supplied a therapeutic level of LCAT into the serum. Because we confirmed the prolonged secretion of LCAT from *lcat*-transduced human ccdPAs over three months (data not shown), the significant reduction in LCAT delivery from transplanted cells at one month or later was probably due to the low cell survival rate at the site of transplantation. Therefore, future studies must focus on the improvement of the cell survival rate and prolong the production of the transgene product *in vivo*.

A clinical trial of an *ex vivo* gene therapy has shown that the implantation of autologous fibroblasts genetically modified to express human nerve growth factor into the forebrain improved the rate of cognitive decline in subjects with Alzheimer disease [40], indicating that the local delivery of therapeutic protein using autologous fibroblasts as a cell vehicle is clinically relevant. The establishment of clinically applicable procedures for the transplantation of gene-transduced human ccdPAs would be useful to obtain further applicable autologous cells for *ex vivo* gene therapy in patients with serum protein deficiencies who require long-term therapeutic protein supplements. In this study, we have analyzed the LCAT secretion property of *lcat* gene-transduced ccdPA from healthy volunteers. The propagated cells from different origins showed the LCAT protein secretion enough for our therapeutic strategy. To further expand our therapeutic strategy for the supplementation of other proteins, it is required to evaluate the characteristics of ccdPA from various kinds of fat diseases such as metabolic syndrome which may affect the secretion function of adipose tissues.

ACKNOWLEDGEMENTS

We thank Atsuo Waki, Kaori Yoshida, Isamu Wakamatsu, Junichi Fukuchi, Kunihiko Ohfuji, Kozo Takamoto, Anna Kakezuka, Mihoko Hatase, Chiho Hattori, Miyuki Ito, Hiroshi Saito, Shohei Akahane, Naomi Kobayashi, Hiromi Harada, Hidemi Sato, Masanori Niimura, Koji Arakawa, Sakura Sekiguchi, Yuko Osa, Koji Fukuda, Reiko Sato, and Rie Ueda, previous members of research division in Cell-GenTech, Inc., for excellent biochemical analysis and valuable discussions. This study was supported in part by Health and Labour Sciences Research Grants for Translational Research, Japan (H. B.).

REFERENCES

[1] Reiser J, Zhang XY, Hemenway CS, Mondal D, Pradhan L, La Russa VF. Potential of mesenchymal stem cells in gene therapy approaches for inherited and acquired diseases. Expert Opin Biol Ther 2005; 5: 1571-84.

[2] Kumar S, Chanda D, Ponnazhagan S. Therapeutic potential of genetically modified mesenchymal stem cells. Gene Ther 2008; 15: 711-5.

[3] Allay JA, Dennis JE, Haynesworth SE, *et al.* LacZ and interleukin-3 expression *in vivo* after retroviral transduction of marrow-derived human osteogenic mesenchymal progenitors. Hum Gene Ther 1997; 8: 1417-27.

[4] Chuah MK, Van Damme A, Zwinnen H, *et al.* Long-term persistence of human bone marrow stromal cells transduced with factor VIII-retroviral vectors and transient production of therapeutic lev-

els of human factor VIII in nonmyeloablated immunodeficient mice. Hum Gene Ther 2000; 11: 729-38.

[5] Lee K, Majumdar MK, Buyaner D, Hendricks JK, Pittenger MF, Mosca JD. Human mesenchymal stem cells maintain transgene expression during expansion and differentiation. Mol Ther 2001; 3: 857-66.

[6] Krebsbach PH, Zhang K, Malik AK, Kurachi K. Bone marrow stromal cells as a genetic platform for systemic delivery of therapeutic proteins *in vivo*: human factor IX model. J Gene Med 2003; 5: 11-7.

[7] Van Damme A, Chuah MK, Dell'accio F, *et al.* Bone marrow mesenchymal cells for haemophilia A gene therapy using retroviral vectors with modified long-terminal repeats. Haemophilia 2003; 9: 94-103.

[8] Kitagawa Y, Bujo H, Takahashi K, *et al.* Impaired glucose tolerance is accompanied by decreased insulin sensitivity in tissues of mice implanted with cells that overexpress resistin. Diabetologia 2004; 47: 1847-53.

[9] Eliopoulos N, Lejeune L, Martineau D, Galipeau J. Human-compatible collagen matrix for prolonged and reversible systemic delivery of erythropoietin in mice from gene-modified marrow stromal cells. Mol Ther 2004; 10: 741-8.

[10] Ito M, Bujo H, Takahashi K, Arai T, Tanaka I, Saito Y. Implantation of primary cultured adipocytes that secrete insulin modifies blood glucose levels in diabetic mice. Diabetologia 2005; 48: 1614-20.

[11] Santamarina-Fojo S, Hoeg JM, Assman G, Brewer HB Jr. Lecithin cholesterol acyltransferase deficiency and fish eye disease. In: Scriver CR, Beaudet AL, Sly WS, Valle D, Childs B, Kinzler KW, Volkman BF (eds). In: The metabolic and molecular bases of inherited disease, 8th Ed. (McGraw-Hill Inc., New York) 2001; 2817-33.

[12] Norum KR, Gjone E. The effect of plasma transfusion on the plasma cholesterol esters in patients with familial plasma lecithin: cholesterol acyltransferase deficiency. Scand J Clin Lab Invest 1968; 22: 339-42.

[13] Murayama N, Asano Y, Kato K, *et al.* Effects of plasma infusion on plasma lipids, apoproteins and plasma enzyme activities in familial lecithin:cholesterol acyltransferase deficiency. Eur J Clin Invest 1984; 14: 122-9.

[14] Casteilla L, Cousin B, Planat-Benard V, Laharrague P, Carmona M, Pénicaud L. Virus-based gene transfer approaches and adipose tissue biology. Curr Gene Ther 2008; 8: 79-87.

[15] Fraser JK, Wulur I, Alfonso Z, Hedrick MH. Fat tissue: an underappreciated source of stem cells for biotechnology. Trends Biotechnol 2006; 24: 150-4.

[16] Gomillion CT, Burg KJ. Stem cells and adipose tissue engineering. Biomaterials 2006; 27: 6052-63.

[17] Zuk PA, Zhu M, Mizuno H, *et al.* Multilineage cells from human adipose tissue: implications for cell-based therapies. Tissue Eng 2001; 7: 211-28.

[18] Gimble J, Guilak F. Adipose-derived adult stem cells: isolation, characterization, and differentiation potential. Cytotherapy 2003; 5: 362-9.

[19] Gimble JM, Katz AJ, Bunnell BA. Adipose-derived stem cells for regenerative medicine. Circ Res 2007; 100: 1249-60.

[20] Sugihara H, Yonemitsu N, Miyabara S, Yun K. Primary cultures of unilocular fat cells: characteristics of growth *in vitro* and changes in differentiation properties. Differentiation 1986; 31: 42-9.

[21] Sugihara H, Yonemitsu N, Miyabara S, Toda S. Proliferation of unilocular fat cells in the primary culture. J Lipid Res 1987; 28: 1038-45.

[22] Rogachev VA, Likhacheva A, Vratskikh O, *et al.* Qualitative and quantitative characteristics of the extracellular DNA delivered to the nucleus of a living cell. Cancer Cell Int 2006; 6: 23.

[23] Ishii I, Onozaki R, Takahashi E, *et al.* Regulation of neutral cholesterol esterase activity by phospholipids containing negative charges in substrate liposome. J Lipid Res 1995; 36: 2303-10.

[24] Ito M, Hiramatsu H, Kobayashi K, *et al.* NOD/SCID/γ_c^{null} mouse: an excellent recipient mouse model for engraftment of human cells. Blood 2002; 100: 3175-82.

[25] Festy F, Hoareau L, Bes-Houtmann S, *et al.* Surface protein expression between human adipose tissue-derived stromal cells and mature adipocytes. Histochem Cell Biol 2005; 124: 113-21.

[26] Rubio D, Garcia-Castro J, Martín MC, *et al.* Spontaneous human adult stem cell transformation. Cancer Res 2005; 65: 3035-9.

[27] Ning H, Liu G, Lin G, *et al.* Identification of an aberrant cell line among human adipose tissue-derived stem cell isolates. Differentiation 2009; 77: 172-80.

[28] Gronthos S, Franklin DM, Leddy HA, Robey PG, Storms RW, Gimble JM. Surface protein characterization of human adipose tissue-derived stromal cells. J Cell Physiol 2001; 189: 54-63.

[29] Zuk PA, Zhu M, Ashjian P, *et al.* Human adipose tissue is a source of multipotent stem cells. Mol Biol Cell 2002; 13: 4279-95.

[30] Yoshimura K, Shigeura T, Matsumoto D, *et al.* Characterization of freshly isolated and cultured cells derived from the fatty and fluid portions of liposuction aspirates. J Cell Physiol 2006; 208: 64-76.

[31] Miyazaki T, Kitagawa Y, Toriyama K, Kobori M, Torii S. Isolation of two human fibroblastic cell populations with multiple but distinct potential of mesenchymal differentiation by ceiling culture of mature fat cells from subcutaneous adipose tissue. Differentiation 2005; 73: 69-78.

[32] Matsumoto T, Kano K, Kondo D, *et al.* Mature adipocyte-derived dedifferentiated fat cells exhibit multilineage potential. J Cell Physiol 2008; 215: 210-22.

[33] Schwarz EJ, Alexander GM, Prockop DJ, Azizi SA. Multipotential marrow stromal cells transduced to produce L-DOPA: engraftment in a rat model of Parkinson disease. Hum Gene Ther 1999; 10: 2539-49.

[34] Chuah MK, Brems H, Vanslembrouck V, Collen D, Vandendriessche T. Bone marrow stromal cells as targets for gene therapy of hemophilia A. Hum Gene Ther 1998; 9: 353-65.

[35] Chiang GG, Rubin HL, Cherington V, *et al.* Bone marrow stromal cell-mediated gene therapy for hemophilia A: *in vitro* expression of human factor VIII with high biological activity requires the inclusion of the proteolytic site at amino acid 1648. Hum Gene Ther 1999; 10: 61-76.

[36] Yu SS, Kim JM, Kim S. High efficiency retroviral vectors that contain no viral coding sequences. Gene Ther 2000; 7: 797-804.

[37] Sakuma M, Akanuma Y, Kodama T, *et al.* Familial plasma lecithin:cholesterol acyltransferase deficiency. A new family with partial LCAT activity. Acta Med Scand 1982: 212: 225-32.

[38] Maeda E, Naka Y, Matozaki T, *et al.* Lecithin-cholesterol acyltransferase (LCAT) deficiency with a missense mutation in exon 6 of the LCAT gene. Biochem Biophys Res Commun 1991; 178: 460-6.

[39] Gotoda T, Yamada N, Murase T, *et al.* Differential phenotypic expression by three mutant alleles in familial lecithin:cholesterol acyltransferase deficiency. Lancet 1991; 338: 778-81.

[40] Tuszynski MH, Thal L, Pay M, *et al.* A phase 1 clinical trial of nerve growth factor gene therapy for Alzheimer disease. Nat Med 2005; 11: 551-5.

Molecular Genetics and Metabolism 102 (2011) 229–231

Contents lists available at ScienceDirect

Molecular Genetics and Metabolism

journal homepage: www.elsevier.com/locate/ymgme

Brief Communication

Disturbed apolipoprotein A-I-containing lipoproteins in fish-eye disease are improved by the lecithin:cholesterol acyltransferase produced by gene-transduced adipocytes *in vitro*

Sakiyo Asada [a,b], Masayuki Kuroda [a,b,*], Yasuyuki Aoyagi [a,b], Hideaki Bujo [a], Shigeaki Tanaka [b], Shunichi Konno [b], Masami Tanio [b], Itsuko Ishii [c], Masayuki Aso [b], Yasushi Saito [d]

[a] *Department of Genome Research and Clinical Application, Graduate School of Medicine, Chiba University, Japan*
[b] *CellGenTech, Inc., Japan*
[c] *Graduate School of Pharmaceutical Sciences, Chiba University, Japan*
[d] *Chiba University, Japan*

ARTICLE INFO

Article history:
Received 3 September 2010
Received in revised form 14 October 2010
Accepted 14 October 2010
Available online 20 October 2010

Keywords:
Lecithin:cholesterol acyltransferase
Fish-eye disease
Familial LCAT deficiency
Apolipoprotein A-I
Protein replacement therapy

ABSTRACT

We report the *in vitro* efficacy of recombinant LCAT produced by *lcat* gene-transduced proliferative adipocytes (ccdPA/*lcat*), which has been developed for enzyme replacement therapy. ApoA-I-specific immunodetection in combination with 1D and 2D gel electrophoreses showed that the disturbed high-density lipoprotein subpopulation profile was clearly ameliorated by the *in vitro* incubation with ccdPA/*lcat*-derived recombinant LCAT. Thus, these results using ccdPA/*lcat* strongly suggest the cell implantation could contribute the enzyme replacement for the patients with LCAT deficiency.

1. Introduction

Lecithin:cholesterol acyltransferase (LCAT) plays a central role in the formation and maturation of high-density lipoproteins (HDLs) [1]. Two classes of genetic deficiencies of LCAT have been identified: familial LCAT deficiency (FLD) and fish-eye disease (FED) [2]. We have been developing a long-lasting LCAT replacement therapy via the transplantation of human *lcat* gene-transduced autologous adipocytes in LCAT-deficient patients. In a previous study, we have described a cell preparation procedure and showed LCAT supplementation in mouse model [3]. However, the potential effect of secreted human LCAT on the improvement of disturbed lipoprotein profile and the mechanism how to remodel HDL *in vitro*, should be evaluated in the patient serum with LCAT deficiency. In this study, we examined the effects of the LCAT-containing culture supernatants from human *lcat* gene-transduced adipocytes on the HDL distribution in the FED patient's serum by apolipoprotein A-I (apoA-I) immunodetection in combination with non-denaturing gel electrophoresis.

2. Materials and methods

The study was approved by the Ethics Committee of Chiba University School of Medicine and informed consent was obtained from the patient. Blood sample was obtained from a patient who had a homozygous mutation in the *lcat* gene causing T123I amino acid substitution in the LCAT protein which was described previously to cause the FED phenotype [4]. The patient and his parents profile were presented in Supplementary Table 1.

Human *lcat* gene was transduced into human ccdPA by retroviral vector. The resulting cells (ccdPA/*lcat*) [3] were seeded into T225 flask and grown to confluency in MesenPRO medium (Invitrogen). The medium was changed to 30 ml of OPTI MEM I (Invitrogen) and the cells were further incubated for seven days to collect culture supernatant. The culture supernatant was concentrated to one-fiftieth of the original volume by Amicon Ultra (MWCO = 50 kDa, Millipore). The amount of rLCAT in the concentrated culture medium (rLCAT/ccdPA/*lcat*) was determined by immunoblotting followed by densitometric analysis using commercially available rLCAT (Roar Biomedical, Inc.) as standard. LCAT activity of the concentrated medium was confirmed as described [3].

Abbreviations: LCAT, lecithin:cholesterol acyltransferase; FED, fish-eye disease; FLD, familial LCAT deficiency; apoA-I, apolipoprotein A-I; ccdPA, ceiling culture-derived proliferative adipocyte.

* Corresponding author. Department of Genome Research and Clinical Application, Graduate School of Medicine, Chiba University, 1-8-1, Inohana, Chuo-ku, Chiba, 260-8670, Japan. Fax: +81 43 2262095.
E-mail address: kurodam@faculty.chiba-u.jp (M. Kuroda).

1096-7192/$ – see front matter © 2010 Elsevier Inc. All rights reserved.
doi:10.1016/j.ymgme.2010.10.009

Concentrated medium containing rLCAT/ccdPA/*lcat* was mixed and incubated at 37 °C with patient serum for 24 h. Inactivation of rLCAT was performed by incubation at 56 °C or addition of 5,5′-Dithiobis-(2-nitrobenzoic acid) [5] (DTNB, Sigma-Aldrich). Serum samples were diluted in 31% sucrose, 0.06% EDTA, and 0.01% BPB prior to gel electrophoresis. Samples corresponding to two micro-liters of serum and those corresponding to 0.25 μl of serum were subjected to non-denaturing two-dimensional (2D) gel electrophoresis [6,7] and 1D gel electrophoresis [8], respectively, with minor modifications. Separated serum proteins were transferred to PVDF membrane (Bio-Rad Laboratories Inc.) and apoA-I was detected by immunoblotting using specific antibodies (Calbiochem) followed by reaction with horseradish peroxidase labeled secondary antibodies. The signal was visualized by SuperSignal West Pico Chemiluminescent reagent (Thermo Fisher Scientific Inc.).

Total cholesterol (TC) and free cholesterol (FC) were quantified in the presence and absence of cholesterol esterase respectively using Cholesterol Quantification kit (BioVision). Cholesteryl ester (CE) contents of samples were then calculated by subtracting FC values from TC values.

Data are presented as means ± S.D. Statistical comparisons were made by ANOVA followed by the post hoc Tukey test using SPSS software. P-values of less than 0.05 were considered as significant.

3. Results

2D analysis showed that the HDL subpopulation distribution of FED patient serum is clearly different from that of healthy serum (Fig. 1A-(a), A-(b)). The patient serum was incubated with the cultured supernatant of ccdPA/*lcat* [3] at a final concentration of rLCAT (6.6 μg/ml), which is equivalent to that in a healthy subject [2,9,10]. The apoA-I-containing lipoprotein distribution in the patient serum was drastically shifted to the larger molecular weight region when the cultured supernatant of ccdPA/*lcat* was added (Fig. 1A-(c)) but not when the supernatant of ccdPA without *lcat* gene transduction was added (Fig. 1A-(d)). The effects were diminished by heat-inactivation of the cultured supernatant before incubation with the patient serum (Fig. 1A-(e)).

Using 1D analysis, a noticeable difference in the apoA-I-containing lipoprotein distribution appeared between the patient (Fig. 1B, lane 1) and the normal subject (Fig. 1B, lane 2). ApoA-I-containing HDL particles were shifted to larger sizes following the incubation with the cultured supernatant of ccdPA/*lcat* in a dose-dependent manner (Fig. 1C, lanes 5–7) as well as following the incubation with rLCAT (Roar Biomedical, Inc., Fig. 1C, lane 12). The incubation with the cultured supernatant of ccdPA (without transduced *lcat* gene, lane4) or PBS (lane 11) did not cause any change from the original serum pattern of the patient. The addition of DTNB (lane 8) or pre-heating the cultured supernatant (lane 9) diminished the effects on HDL particle shifting. The addition of the ccdPA/*lcat* cultured supernatant significantly elevated the CE levels in the HDL fractions (Fig. 1D, lane 7), as observed by the addition of rLCAT (Roar Biomedical, Inc., lane 12) and in agreement with the shift observed in 1D gel electrophoresis (Fig. 1C, lane 7). Taken together, the two kinds of gel electrophoresis analysis in combination with immunoblotting demonstrated that the disturbed HDL subpopulation distribution is ameliorated by *in vitro* incubation of the serum with the ccdPA/*lcat*-derived recombinant LCAT in FED patients.

4. Discussion

We have been focusing on adipocytes as a therapeutic protein-secreting vehicle, since adipose tissue is well-vascularized and, secretes many cytokines systemically into the blood stream [11].

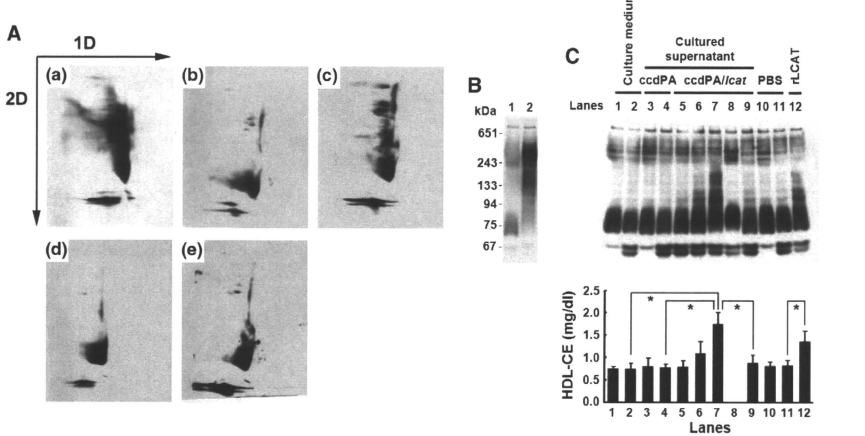

Fig. 1. Analysis of mobility changes in apoA-I-containing particles by *in vitro* incubation with rLCAT. A. Serum samples of normal subjects (a) and FED patient (b, c, d and e) were analyzed by 2D gel electrophoresis followed by immunoblotting against apoA-I. The patient serum without incubation (b). The patient serum was incubated at 37 °C for 24 h with cultured supernatant derived from *lcat* gene-transduced ccdPA (c) or with cultured supernatant from ccdPA (d), or with heat-inactivated cultured supernatant derived from *lcat* gene-transduced ccdPA (e). B. Serum samples of FED patient (lane 1) and normal subject (lane 2) were analyzed by 1D gel electrophoresis followed by immunoblotting against apoA-I. C. Culture medium (lanes 1 and 2), cultured supernatant of untransduced (lanes 3 and 4) or human *lcat* gene-transduced (lanes 5 to 9) ccdPA, phosphate-buffered saline (PBS, lanes 10 and 11), and recombinant LCAT 60 μg/ml (Roar Biomedical, Inc.) (lane 12) were added to the patient serum and incubated at 37 °C for 24 h (lanes 2, 4–9, 11 and 12). Samples without incubation (lanes 1, 3 and 10) were included as controls. Heat inactivated cultured supernatant of human *lcat* gene-transduced ccdPA was used (lane 9). DTNB (2 mM) was included in the reaction mixture (lane 8). The concentrations of ccdPA-derived LCAT in the reaction mixtures were 0.7 (lane 5), 2.2 (lane 6), and 6.6 (lane 7 to 9) μg/ml, respectively. HDL-CE in the reaction mixtures was quantified and shown in the bar graph at the bottom. The quantification of HDL-CE in the sample shown in lane 8 was not performed due to the interference of DTNB with the enzymatic determination of cholesterol [20]. *$p < 0.05$.

The products of exogenous genes reach the circulation when it is overexpressed in the adipocytes after their transplantation in mice, although the precise mechanism is unknown [12–15]. The long-lasting blood glucose-lowering effect upon transplantation of insulin gene-transduced adipocytes by retroviral vector strongly suggested the stable expression of LTR-driven transgene expression in adipocytes [12]. Thus, we have developed retrovirally-*lcat* gene-transduced ccdPA (ccdPA/*lcat*) as a stably LCAT supplying vehicle *in vivo* [3]. The LCAT supplementation was indeed steadily detected in the serum after transplantation for 4 weeks in the adipocyte-transplanted mice [3].

ApoA-I is a cofactor of LCAT, and the proper interaction between them in the serum is required for the proper remodeling of HDL, and the mechanism of LCAT activation by apoA-I is not completely determined [16]. Here, we examined the functional issue to be dissolved before the subsequent clinical application, whether LCAT protein secreted by ccdPA/*lcat* improves the disturbed lipoprotein remodeling in human patient's serum. The 2D analysis of the apoA-I-containing HDL distribution profile showed that the rLCAT changed the abnormal HDL population sizes in the FED patient toward the pattern in the normal subject. This change in the HDL particles was also detected using 1D electrophoresis with the rLCAT-dependent formation of CE in HDL. Thus, the incubation with the rLCAT derived from ccdPA/*lcat* stimulated CE formation and the subsequent maturation of HDL subpopulations in the FED patient serum. Thus, rLCAT from ccdPA/*lcat* is functional in correcting the abnormal HDL distribution in the serum of FED patient. It is still assumed that the rLCAT supplied *in vivo* might not as effective in LCAT-deficient patients as the here shown *in vitro* results, since the tissue supplying the recombinant enzyme is adipocytes, and not the liver, original site producing LCAT, thus causing the presence of unexpected inhibitor(s), inefficient interaction with the patient apoA-I, or accelerated dynamics of the enzyme [17]. A clinical application of ccdPA/*lcat* transplantation is now in progress in Japan as a first clinical trial. Based on the *in vitro* study, the 1D and 2D gel electrophoresis examinations of the HDL profile in the sera of patients are expected to contribute to the clinical evaluation of the treatment efficacy after the cell transplantation, in addition to the *in vitro* functional examination of the patient's ccdPA/*lcat*-derived rLCAT against their own serum prior to the cell transplantation.

Acknowledgment

This study was supported in part by Health and Labour Sciences Research Grants for Translational Research, Japan (H. B.).

Appendix A. Supplementary data

Supplementary data to this article can be found online at doi:10.1016/j.ymgme.2010.10.009.

References

[1] G.F. Lewis, D.J. Rader, New insights into the regulation of HDL metabolism and reverse cholesterol transport, Circ. Res. 96 (2005) 1221–1232.
[2] S. Santamarina-Fojo, J.M. Hoeg, G. Assman, H.B. Brewer Jr., Lecithin cholesterol acyltransferase deficiency and fish eye disease, in: C.R. Scriver, A.L. Beaudet, W.S. Sly, D. Valle, B. Childs, K.W. Kinzler, B.F. Volkman (Eds.), The Metabolic and Molecular Bases of Inherited Disease, 8th Eds., McGraw-Hill Inc., New York, 2001, pp. 2817–2833.
[3] M. Kuroda, Y. Aoyagi, S. Asada, H. Bujo, S. Tanaka, S. Konno, M. Tanio, I Ishii, K. Machida, F. Matsumoto, K. Satoh, M. Aso, Y. Saito, Ceiling culture-derived proliferative adipocytes are a possible delivery vehicle for enzyme replacement therapy in lecithin:cholesterol acyltransferase deficiency. Gene Ther Mol Biol; in press.
[4] H. Funke, A. von Eckardstein, P.H. Pritchard, J.J. Albers, J.J. Kastelein, C. Droste, G. Assmann, A molecular defect causing fish eye disease: an amino acid exchange in lecithin-cholesterol acyltransferase (LCAT) leads to the selective loss of alpha-LCAT activity, Proc. Natl Acad. Sci. USA 88 (1991) 4855–4859.
[5] L. Holmquist, L.A. Carlson, Normalization of high density lipoprotein in fish eye disease plasma by purified normal human lecithin: cholesterol acyltransferase, Lipids 23 (1988) 225–229.
[6] A. von Eckardstein, Y. Huang, S. Wu, H. Funke, G. Noseda, G. Assmann, Reverse cholesterol transport in plasma of patients with different forms of familial HDL deficiency, Arterioscler. Thromb. Vasc. Biol. 15 (1995) 691–703.
[7] B.F. Asztalos, E.J. Schaefer, K.V. Horvath, S. Yamashita, M. Miller, G. Franceschini, L. Calabresi, Role of LCAT in HDL remodeling: investigation of LCAT deficiency states, J. Lipid Res. 48 (2007) 592–599.
[8] Y. Nakamura, L. Kotite, Y. Gan, T.A. Spencer, C.J. Fielding, P.E. Fielding, Molecular mechanism of reverse cholesterol transport: reaction of pre-beta-migrating high-density lipoprotein with plasma lecithin/cholesterol acyltransferase, Biochemistry 43 (2004) 14811–14820.
[9] J.J. Albers, C.H. Chen, J.L. Adolphson, Lecithin:cholesterol acyltransferase (LCAT) mass; its relationship to LCAT activity and cholesterol esterification rate, J. Lipid Res. 22 (1981) 1206–1213.
[10] T. Miida, O. Miyazaki, O. Hanyu, Y. Nakamura, S. Hirayama, I. Narita, F. Gejyo, I. Ei, K. Tasaki, Y. Kohda, T. Ohta, S. Yata, I. Fukamachi, M. Okada, LCAT-dependent conversion of prebeta1-HDL into alpha-migrating HDL is severely delayed in hemodialysis patients, J. Am. Soc. Nephrol. 14 (2003) 732–738.
[11] T. Ronti, G. Lupattelli, E. Mannarino, The endocrine function of adipose tissue: an update, Clin. Endocrinol. 64 (2006) 355–365.
[12] M. Ito, H. Bujo, K. Takahashi, T. Arai, I. Tanaka, Y. Saito, Implantation of primary cultured adipocytes that secrete insulin modifies blood glucose levels in diabetic mice, Diabetologia 48 (2005) 1614–1620.
[13] M. Shibasaki, H. Bujo, K. Takahashi, K. Murakami, H. Unoki, Y. Saito, Catalytically inactive lipoprotein lipase overexpression increases insulin sensitivity in mice, Horm. Metab. Res. 38 (2006) 491–496.
[14] Y. Kitagawa, H. Bujo, K. Takahashi, M. Shibasaki, K. Ishikawa, K. Yagui, N. Hashimoto, K. Noda, T. Nakamura, S. Yano, Y. Saito, Impaired glucose tolerance is accompanied by decreased insulin sensitivity in tissues of mice implanted with cells that overexpress resistin, Diabetologia 47 (2004) 1847–1853.
[15] Y. Kubota, H. Unoki, H. Bujo, N. Rikihisa, A. Udagawa, S. Yoshimoto, M. Ichinose, Y. Saito, Low-dose GH supplementation reduces the TLR2 and TNF-alpha expressions in visceral fat, Biochem. Biophys. Res. Commun. 368 (2008) 81–87.
[16] M.G. Sorci-Thomas, S. Bhat, M.J. Thomas, Activation of lecithin:cholesterol acyltransferase by HDL ApoA-I central helices, Clin. Lipidol. 4 (2009) 113–124.
[17] A. Jonas, Lecithin cholesterol acyltransferase, Biochim. Biophys. Acta 1529 (2000) 245–256.
[18] M. Manabe, T. Abe, M. Nozawa, A. Maki, M. Hirata, H. Itakura, H, New substrate for determination of serum lecithin:cholesterol acyltransferase, J. Lipid Res. 28 (1987) 1206–1215.
[19] K. Taira, H. Bujo, J. Kobayashi, K. Takahashi, A. Miyazaki, Y. Saito, Positive family history for coronary heart disease and 'midband lipoproteins' are potential risk factors of carotid atherosclerosis in familial hypercholesterolemia, Atherosclerosis 160 (2002) 391–397.
[20] W.S. Harris, A. Rayford, LCAT inhibitors interfere with the enzymatic determination of cholesterol and triglycerides, Lipids 25 (1990) 341–343.

① 外傷性裂開創(一次閉鎖が不可能なもの)
② 外科手術後離開創・開放創
③ 四肢切断端開放創
④ デブリードマン後皮膚欠損創

とされるが，具体的には急性創傷ではデグロービング外傷，開放性骨折，術後創離開，術後開放創など，慢性創傷では褥瘡，糖尿病性足壊疽など，真皮よりも深い創傷でデブリードマン後の創傷が対象となる．

NPWT のシステムの特徴から創傷を密閉することになるので，感染創を対象とする際にはあらかじめ壊死組織除去や抗菌薬などを使用し，感染を制御しておくことが推奨される．

また，露出した血管，臓器に直接 NPWT を使用することは大出血や重大事故につながるおそれがあるため，禁忌とされる．

NPWTの応用

NPWT はコラーゲン使用人工皮膚や持続洗浄とともに用いても効果を発揮する．

NPWT に，ドレーン孔を有するコラーゲン使用人工真皮(テルダーミス真皮欠損用グラフト®膜付きドレーン孔タイプ，東京，オリンパステルモバイオマテリアル社)を併用する方法では，肉芽形成をさらに促進することが可能である．

持続洗浄と NPWT の組合せでは洗浄によって感染を制御しながら陰圧を負荷できるので，感染を認める創傷における NPWT の可能性を拡大させる[3]．

褥瘡などの慢性創傷において皮弁移植術を計画する場合には，NPWT を術前に施行することで創傷を最適な状態へ変換し，周術期合併症の発生リスクを軽減することが可能となる[2]．

また，網状分層植皮術における固定用のドレッシング材としても有用である．

おわりに

V. A. C. に代表される NPWT は難治性潰瘍に対する確立された治療法として，いまや世界的に認知されている．わが国においても完成度の高い V. A. C. の登場は，創傷の臨床医に NPWT の効果を再認識させ，多くの難治性潰瘍をもつ患者に光明をもたらすことになるであろう．

1) Argenta, L. C. and Morykwas, M. J.：Vacuum-assisted closure：a new method for wound control and treatment：clinical experience. *Ann. Plast. Surg.*, **38**：563-576, 1997.
2) 大浦紀彦・他：【難治性潰瘍の新しい治療法】陰圧閉鎖療法について．形成外科，**52**：903-912, 2009.
3) Kiyokawa, K. et al.：New continuous negative-pressure and irrigation treatment for infected wounds and intractable ulcers. *Plast. Reconstr. Surg.*, **120**：1257-1265, 2007.

大浦紀彦，波利井清紀／
Norihiko OHURA and Kiyonori HARII
杏林大学医学部形成外科

糖尿病・内分泌代謝学

脂肪細胞による新規蛋白質補充療法

——LCAT欠損症遺伝子治療臨床研究

Enzyme replacement therapy by gene-transduced adipocytes for LCAT deficiency

LCAT 欠損症やライソゾーム病などの難治性遺伝病には，根治療法が存在しない．これらの希少疾患の生命予後や生活を改善するための持続的な蛋白質補充を行う手段として，安全で普遍的，また医療経済に適合した細胞治療法があげられる．このような考えから著者らは，すでに日常臨床で安全に行われている皮下脂肪組織の摘出と脂肪細胞の移植技術を基盤にした新規の細胞治療法を開発した(図 1)[1]．この特徴は，これまでの多くの研究で得られてきた脂肪細胞の多彩な機能と生体における安定性を，遺伝子導入細胞として応用することにある．本稿では，本治療法による LCAT 欠損症治療実用化開発を概説する．

LCAT欠損症とは

レシチン：コレステロールアシルトランスフェラーゼ(LCAT)はリポ蛋白 HDL とともに存在し，血中コレステロールのエステル化を担う酵素である．LCAT 欠損症は，まれな常染色体劣性遺伝性疾患である．北ヨーロッパ，日本を中心に本疾患患者が同定され，原因となる 40 種類以上の LCAT 遺伝子異常が報告されている．低 HDL 血症とともに角膜混濁，溶血性貧血，腎不全などの臨床症状を呈し，根治療法は存在しない[2]．新鮮血漿の輸血により一時的に臨床症状が改善したという報告[3,4]があることから，長期間安定に持続する LCAT 補充療法が期待される．

自己移植用脂肪細胞 ccdPA[5]

形成外科領域で一般に行われる臨床技術である脂肪吸引により得られる脂肪組織から，遺伝子導入用脂肪細胞を調製することができる．脂肪細胞は油滴を含むために比重が小さいことがこの調製に利用される．脂肪組織をコラゲナーゼ処理し遠心後の沈渣(stromal vascular fraction：SVF)を除き，他の細胞などの含まれない成熟脂肪細胞分画を収集することができる．この油滴含有脂肪細胞分画を用いて天井培養法[6]により遺伝子導入用細胞(ceiling culture-derived

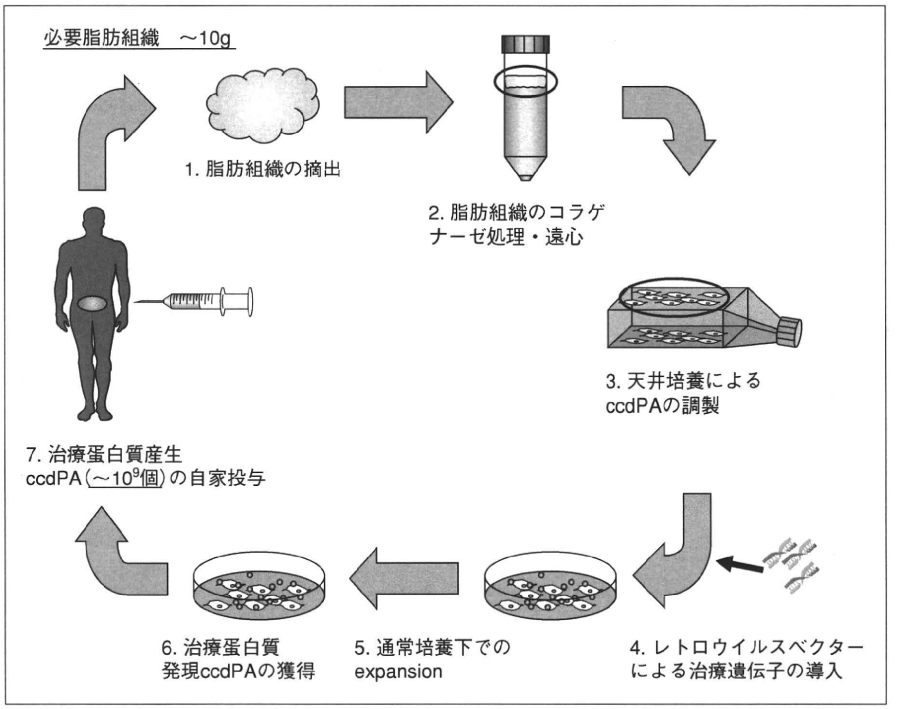

図 1　遺伝子導入脂肪細胞を用いた蛋白質補充療法の概略

患者腹部脂肪組織を摘出し，天井培養により遺伝子導入用脂肪細胞(ccdPA)を獲得する．レトロウイルスベクターによる治療用遺伝子導入の後，拡大培養した細胞を回収し，腹部脂肪組織に自己移植する．1回の治療に必要な移植用 ccdPA は脂肪組織摘出後3週間で調製される．

proliferative adipocytes：ccdPA)が調製される．SVF には多分化能を有する幹細胞が存在するのに対し[7]，ccdPA はこれらが排除され，表面蛋白プロファイルの安定な細胞の集団となる．ccdPA は線維芽細胞様の形態を示し，脂肪細胞への成熟能が優れる．一部で SVF 由来幹細胞が長期 *ex vivo* 培養によりトランスフォーム(癌化)する報告があるのに対し[8]，ccdPA はこれまで異常増殖の所見は認められておらず，移植治療において安全性に優れた細胞と考えられる．

ccdPAによるLCAT補充

ccdPA にレトロウイルスベクターを用いて遺伝子導入を行うと，高陽性率(40～50%)，低平均導入コピー数(細胞当り約 1 コピー)と，遺伝子治療用の細胞として理想的な細胞であることが示される[5]．LCAT 遺伝子導入 ccdPA は，正常 LCAT と同等のコレステロールエステル化活性を有する酵素蛋白を培地中に分泌する[5]．LCAT 欠損症患者血清にこの分泌 LCAT を添加作用させるとエステル化障害による異常なリポ蛋白が是正され，正常な分布に近づく．LCAT 遺伝子導入 ccdPA をマウスに移植すると，全身のリポ蛋白代謝を改善することが期待できる LCAT 蛋白が血中に補充された．またこの効果は，すくなくとも数カ月持続することが予想される．

おわりに

LCAT 欠損症患者を対象にした遺伝子治療臨床研究“家族性 LCAT 欠損症を対象とした LCAT 遺伝子導入ヒト前脂肪細胞の自家移植に関する臨床研究”は，千葉大学医学部附属病院遺伝子治療臨床研究審査委員会での承認を得，平成 22 年 (2010) 4 月，厚生労働省へ実施申請書類を提出した．今後は LCAT 欠損症に加えて，さまざまな蛋白欠損症(酵素欠損症，血友病，糖尿病など)を対象に，その合併症が進行することを抑制できる新規細胞治療法として広く臨床応用されることが期待される．

謝辞：本研究は千葉大学(齋藤康学長)，セルジェンテック株式会社(麻生雅是社長)との共同研究により実施されたものである．

1) Ito, M. et al.：Implantation of primary cultured adipocytes that secrete insulin modifies blood glucose levels in diabetic mice. *Diabetologia*, **48**：1614-1620, 2005.
2) Santamarina-Fojo, S. et al.：Lecithin cholesterol acyltransferase deficiency and fish eye disease. *In*：The Metabolic and Molecular Bases of Inherited Disease, 8th ed.(ed. by Scriver, C. R. et al.). McGraw-Hill, New

York, 2001, pp.2817-2833.
3) Norum, K. R. and Gjone, E.: The effect of plasma transfusion on the plasma cholesterol esters in patients with familial plasma lecithin: cholesterol acyltransferase deficiency. *Scand. J. Clin. Lab. Invest.*, **22**: 339-242, 1968.
4) Murayama, N. et al.: Effects of plasma infusion on plasma lipids, apoproteins and plasma enzyme activities in familial lecithin: cholesterol acyltransferase deficiency. *Eur. J. Clin. Invest.*, **14**: 122-129, 1984.
5) Kuroda, M. et al.: Ceiling culture-derived proliferative adipocytes are a possible delivery vehicle for enzyme replacement therapy in lecithin: cholesterol acyltransferase deficiency. *Gene Ther. Mol. Biol.*, 2010.(in press)
6) Sugihara, H. et al.: Primary cultures of unilocular fat cells: characteristics of growth *in vitro* and changes in differentiation properties. *Differentiation*, **31**: 42-49, 1986.
7) Gimble, J. M. et al.: Adipose-derived stem cells for regenerative medicine. *Circ. Res.*, **100**: 1249-1260, 2007.
8) Rubio, D. et al.: Spontaneous human adult stem cell transformation. *Cancer Res.*, **65**: 3035-3039, 2005.

黒田正幸，武城英明／
Masayuki KURODA[1] and Hideaki BUJO[2]
千葉大学医学部附属病院糖尿病・代謝・内分泌内科[1]，同大学院医学研究院臨床遺伝子応用医学[2]

泌尿器科学

最新の膀胱癌初期治療

——病理の視点から

An updated initial treatment for bladder cancer
——From a pathological point of view

膀胱癌は初期症状が乏しく，進行癌で発見されることもまれではない．加えて，前立腺癌の PSA (prostatic specific antigen)に相当するような有用なスクリーニングのマーカーがなく，尿細胞診がもっとも有効・簡便で安価な検出法として定着している．欧米では尿検体を用いた FISH(fluorescence *in situ* hybridization)法(UroVysion, Abbott)が尿細胞診よりも精度がよい(高感度)との報告から実用化されているが，コストの問題などからわが国での導入は研究レベルの段階である．一方，膀胱癌の病理組織学的診断および治療の目的で行われる TUR(transurethral resection)に関しては，1990 年代から T1 high grade 腫瘍(粘膜固有層浸潤があるが，筋層浸潤のない high grade の膀胱癌)に対する second TUR の重要性が提唱されている．ここでは膀胱癌の初期治療の際に，尿細胞診と病理の情報をいかに有効に活用するかについて解説する．

尿細胞診でどこまでわかるか

尿細胞診は尿中に剝離した腫瘍細胞を顕微鏡で観察して診断する方法で，尿路上皮癌に対する感度はおよそ 40〜60%，特異度は 90〜100%である．grade 1 の尿路上皮癌では細胞が剝離しにくいために尿細胞診の感度は約 10%と低いが，grade 3 や上皮内癌の感度は 70%を超える．つまり緊急性の高い高異型度尿路上皮癌の多くは，尿細胞診で検出可能である．

尿細胞診で予測可能な病理所見としては，①grade，②組織型，③浸潤の有無がある．さらに，扁平上皮や腺管への分化を示すもの，および micropapillary variant, plasmacytoid variant など粘膜固有層浸潤以上(T1 以上)の可能性がきわめて高い組織亜型も細胞診で予測可能なことがある．壊死性の背景は，通常は T1 以上の浸潤癌でのみ認められる．

病理標本でどこまでわかるか

病理に提出される TUR 検体は，大きく 2 つに分けられる．1 つは腫瘍のサイズが比較的小さく，粘膜面と垂直方向に腫瘍組織を切出すことが可能な適切な検体

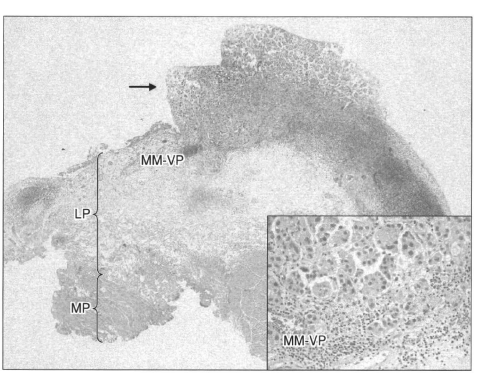

図 1　固有筋層(MP)を含み，垂直方向に切り出された適切な病理標本
pT1 high grade, micropapillary variant の尿路上皮癌(矢印)で粘膜固有層(LP)内の粘膜筋板(MM)-血管叢(VP)に浸潤がある．右下は腫瘍の中拡大像．深部断端は陰性．Second TUR は必要であろうか？

Original Article

Contradictory Effects of β1- and α1- Aderenergic Receptor Blockers on Cardio-Ankle Vascular Stiffness Index (CAVI)

— CAVI is Independent of Blood Pressure —

Kohji Shirai[1], Mingling Song[1,2], Jun Suzuki[3], Takumi Kurosu[3], Tomokazu Oyama[1], Daiji Nagayama[1], Yoh Miyashita[1], Shigeo Yamamura[4], and Mao Takahashi[1]

[1]Internal Medicine, Sakura Hospital, School of Medicine, Toho University, Chiba, Japan
[2]Endocrinological Division, Ikai City Hospital, Ikai, China
[3]Physiological Department, Sakura Hospital, School of Medicine, Toho University, Chiba, Japan
[4]Faculty of Pharmaceutical Sciences Josai International University, Chiba, Japan

Aim: The cardio-ankle vascular stiffness index (CAVI) is a new parameter that reflects the stiffness of the aorta, femoral artery and tibial artery as a whole. One of its conspicuous features is that CAVI is independent of blood pressure at measuring time, theoretically. But, it has not been experimentally proved yet. For confirmation, pharmacological studies were performed comparing with brachial-ankle pulse wave velocity (baPWV).

Methods: Used drugs were a β1-adrenoceptor blocker, metoprorol and an α1- adrenoceptor blocker doxazosin. Both were administered to 12 healthy volunteer men. CAVI and baPWV were measured every one hour for 6 hours using VaSera.

Results: When metoprolol (80 mg) was administered to 12 healthy volunteer men, systolic blood pressure decreased from 131.4±4.5 to118.3±4.1 mmHg (mean±SE) ($p<0.05$) at the 3rd hour, and diastolic blood pressure decreased from 85.3±4.0 to 75.3±3.0mmHg ($p<0.05$). baPWV decreased from 13.93±0.46 to 12.46±0.49 m/sec ($p<0.05$), significantly, but CAVI did not change (8.16±0.29 to 8.24±0.27) ($p=0.449$). ΔbaPWV at each time was significantly correlated with both Δsystolic and Δdiastolic blood pressures, but ΔCAVI was not correlated with either Δblood pressure. When doxazosin (4 mg) was administered to the same men, systolic blood pressure decreased from 130.2±4.6 to117.2±4.8 mmHg ($p<0.05$) at the 3rd hour. Diastolic blood pressure also decreased from 85.1±4.1 to 74.2±3.9 mmHg ($p<0.05$). baPWV decreased from 13.98±0.68 to 12.25±0.53 m/sec ($p<0.05$), significantly. CAVI also decreased from 8.15±0.28 to 7.18±0.37 ($p<0.05$), significantly.

Conclusion: These results suggested that CAVI was not affected by blood pressure at the measuring time directly, but affected by the changes of contractility of smooth muscle cells.

J Atheroscler Thromb, 2011; 18:49-55.

Key words; Cardio-ankle vascular stiffness index, CAVI, Arterial stiffness, α1-Antagonist, Doxazosin, β1-Antagonist, Metoprolol, Blood pressure

Address for Correspondence: Kohji Shirai, Department of Internal Medicine, Sakura Hospital, School of Medicine, Toho University, 564-1 Shimoshizu, Sakura-shi, Chiba Prefecture, 285, Japan
E-mail: kshirai@kb3.so-net.ne.jp
Received: August 8, 2009
Accepted for publication: August 31, 2010

Introduction

Measuring arterial stiffness would provide valuable information about arterial wall conditions, which include sclerosis and contraction of arterial smooth muscles[1]. Several parameters reflecting arterial stiffness have been proposed, including pulse wave velocity (PWV)[2-4]. The importance of measuring PWV as a marker of arteriosclerosis was pointed out[5,6]. In 1990,

baPWV was proposed[7] and its utility as a predictive marker of multiple coronary artery occlusive disease was reported[8]. However, it has been reported that PWV depends on blood pressure at the time of measurement[5]. It is therefore difficult to know the real arterial stiffness by measuring PWV, and it is also inadequate to evaluate the effect of controlling hypertension with blood pressure-lowering agents on arterial wall condition itself. Hasegawa and coworkers[9] proposed corrected aortic PWV (cPWV), which reflects PWV from the origin of the aorta to the femoral artery. They made a monograph to correct aortic PWV for diastolic blood pressure adjusted to 80 mmHg. The utility of cPWV has been mentioned[10, 11]. However, this method does not reflect arterial stiffness directly and has problems detecting the pulse of the femoral artery in the inguinal area.

In 2006, a new blood pressure-independent arterial wall stiffness parameter, the cardio-ankle vascular stiffness index (CAVI), was proposed[12]. The properties of CAVI[13, 14] and its clinical significance for diabetes mellitus[15], carotid arteriosclerosis, hypertension[16], coronary arterial disease[17] and renal disease [18, 19] were reported recently, suggesting that CAVI increased in arteriosclerotic diseases and was scarcely affected by blood pressure[12, 15].

Theoretically, CAVI is independent of blood pressure at the time of measurement[12], because CAVI is essentially originated from stiffness parameter beta[20, 21]. But, it has not been experimentally proved yet.

To address this, we studied CAVI changes while the blood pressure was changed using two agents with different mechanisms to lower blood pressure. One is β1- adrenergic receptor blocker. β-1 Adrenergic receptor exists in the heart muscle and enhances the contraction and the pulse of the heart[22, 23]. We chose metoprolol as the β1 selective blocker[23]. It is supposed to decrease blood pressure by reducing heart muscle contraction, not by vasodilation. If CAVI would be dependent on blood pressure at the measuring time, CAVI would decrease when blood pressure decreased by β-1 blocker.

The other used agent was α-1 adrenergic receptor blocker. α-1 Adrenergic receptor exists in vascular smooth muscle cells and induces contraction of the artery wall and raises the blood pressure[24, 25]. As the α-1 selective blocker, we chose doxazosin[25]. Doxazosin inhibits the binding of norepinephrine to α-1 adrenergic receptor in vascular smooth muscle cells, resultantly relaxing vascular smooth muscle cell tone, which decreases peripheral vascular resistance, leading to a decrease in blood pressure[24, 25]. In this case, CAVI would be expected to decrease.

For these confirmations, both agents were administered to healthy 12 volunteer men alternatively at 7-day intervals. CAVI and baPWV were measured every hour for 6 hours, simultaneously. The correlations between the changes of CAVI or of baPWV (ΔCAVI or ΔbaPWV = value before − value at each time, respectively), and blood pressure changes (ΔBP = value before − value at each time) during the administration of both agents were also studied.

Subjects and Methods

Subjects

The subjects were 12 male volunteers aged from 40 to 60 years (mean ± SE 47 ± 5). They were essentially healthy without diabetes mellitus and hypertension, and were not taking any drugs. This study was approved by the Research Ethics Board at Sakura Hospital, Toho University. Informed consent was given and the consensus was obtained. They were administered 80 mg of metoprolol, 2 hours after breakfast. CAVI and baPWV were measured every hour for 6 hours in the supine position after a 10-minute rest each time. During the interval between measuring times, they rested in a sitting position and were prohibited to smoke and exercise. One week later, the same men were administered 4 mg doxazosin and CAVI and baPWV were measured in the same manner.

Measuring CAVI and baPWV

At measuring, a 10-minute rest was taken in the supine position. The precise methods were described in the previous report[12]. Briefly, to detect brachial and ankle pulse waves using cuffs, cuff pressure was from 30 mmHg to 50 mmHg, to ensure the minimal effect of cuff pressure on hemodynamics. Blood pressure was measured after detecting the pulse.

CAVI is determined by the following equation

$$CAVI = a\{(2\rho/\Delta P) \times \ln(Ps/Pd)\ PWV^2\} + b$$

Where Ps and Pd are systolic and diastolic blood pressures, PWV is pulse wave velocity from the origin of the aorta to the junction of the tibial artery with the femoral artery, ΔP is Ps − Pd, ρ is blood density, and a and b are constants. CAVI is derived from β ($\beta = \ln(Ps/Pd) \cdot D/\Delta D$)[20, 21], and D/$\Delta$D is drawn from the modification of Bramwell-Hill's equation[2].

baPWV was calculated simultaneously[7].

These measuring tools and calculation system were equipped in VaSera (Fukuda Denshi Co. Ltd, Tokyo).

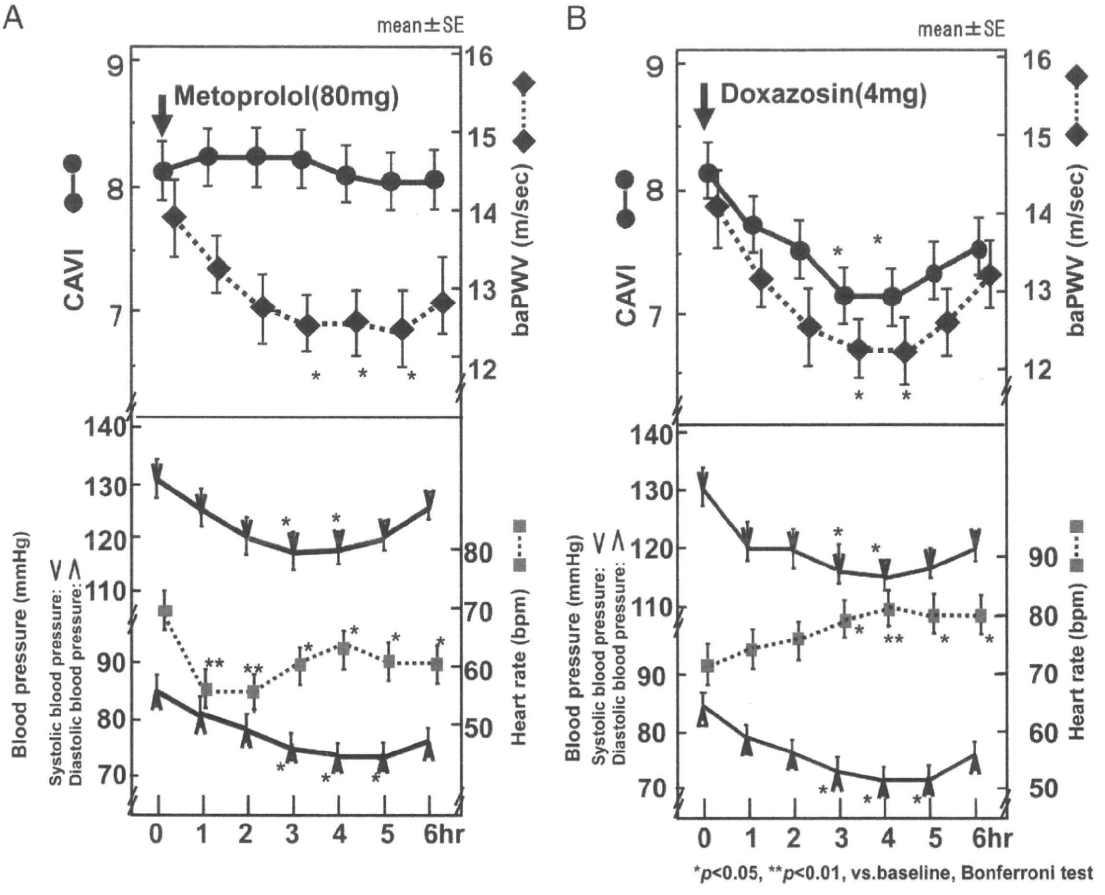

Fig. 1.

A.Effects of metoprolol on CAVI, baPWV, blood pressures and heart rate
Metoprolol (80 mg) was administered to 12 men. CAVI, baPWV, systolic blood pressure, diastolic blood pressure and heart rate were measured every hour for 6 hours.

B.Effects of doxazosin on CAVI, baPWV, blood pressure and pulse rate
Doxazosin (4 mg) was administered to 12 men. CAVI, baPWV, systolic blood pressure, diastolic blood pressure and heart rate were measured every hour for 6 hours.

Statistical analysis

The data are presented as the mean ± SE. The difference in response curves at each time point from baseline was determined by the two-tailed multiple *t*-test with Bonferroni correction following one-way ANOVA.

The correlations between ΔCAVI or ΔbaPWV, and Δsystolic blood pressure or Δdiastolic pressure were analyzed by Spearman's correlation coefficient analysis. Significance was less than $p=0.05$.

Results

1. Effect of metoprolol administration on blood pressure, baPWV and CAVI (Fig. 1A)

Metoprolol (80 mg) was administered to 12 men. Systolic blood pressure started to decrease at 1 hour from 131.4 ± 4.5 to 118.3 ± 4.1 mmHg (mean ± SE) ($p<0.05$) at 3 hour and the decrease continued for 5 hours.

Diastolic blood pressure also started to decrease at 1 hour from 85.3 ± 4.0 to 75.3 ± 3.0 mmHg ($p<0.05$) at 3 hours. The decrease continued for 6 hours.

Heart rate decreased from 70.25 ± 3.3 /min to 55.92 ± 1.8 /min at 2 hours, and returned slightly (60.4 ± 1.8 /min at 3 hours). This low heart rate continued for 6 hours.

baPWV started to decrease at 1 hour from 13.93 ± 0.46 m/sec to 12.46 ± 0.49 m/sec ($p<0.05$) at 3 hours, significantly.

CAVI increased slightly from 8.16 ± 0.29 to 8.23 ± 0.28 at 2 hours and to 8.24 ± 0.27 at 3 hours, then

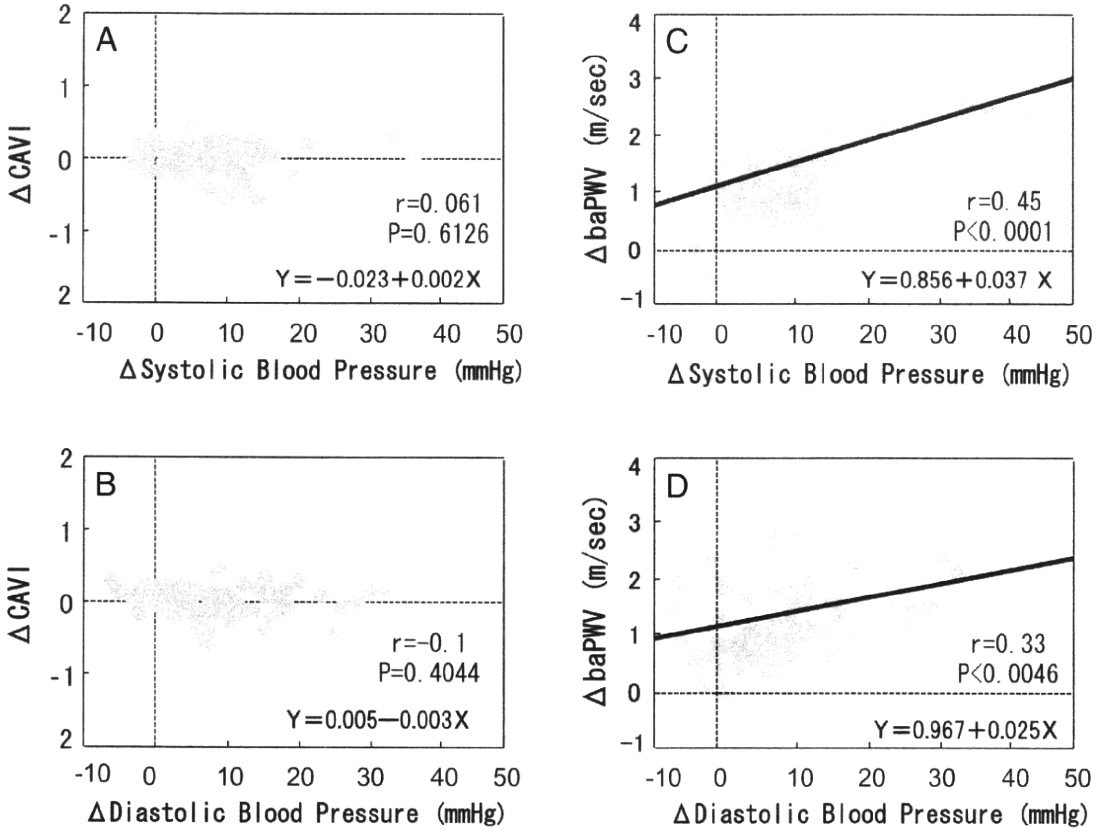

Fig. 2. Correlations between ΔCAVI and ΔbaPWV, and Δblood pressures during metoprolol administration

The differences in vascular parameters (Δ) between before and after metoprolol administration each hour were calculated and their correlation shown.

A, B: Correlations between ΔCAVI, and Δsystolic pressure (A) and Δdiastolic pressure (B) during metoprolol administration

C, D: Correlations between ΔbaPWV, and Δsystolic pressure (C) and Δdiastolic pressure (D) during metoprolol administration

decreased slightly to 8.10 ± 0.27 at 5 hours (p=0.449), however, these changes were not statistically significant.

The differences in vascular parameters (Δ) between before and after metoprolol administration at each hour were calculated and the correlations are shown in **Fig. 2**. As shown in **Fig. 2C, D**, ΔbaPWV and Δsystolic blood pressure were significantly correlated (ΔPWV=0.856+0.037×ΔsBP, r=0.45, p< 0.0001), and, ΔbaPWV and Δdiastolic blood pressure were also correlated significantly (ΔPWV=0.967+ 0.025×ΔdBP, r=0.33, p=0.0046).

The correlation between ΔCAVI and Δsystolic blood pressure and Δdiastolic blood pressure during metoprolol administration is shown in **Fig. 2A, B**. ΔCAVI and Δsystolic blood pressure were not correlated (ΔCAVI=−0.023+0.002×ΔsBP, r=0.061, p=0.61). ΔCAVI and Δdiastolic blood pressure were also not correlated (ΔCAVI=0.005−0.003×ΔdBP, r=−0.100, p=0.4044)

ΔbaPWV and Δheart rate were correlated (ΔbaPWV=1.014+0.018×ΔHR, r=0.235, p=0.047, data not shown). ΔCAVI and Δheart rate were not correlated (ΔCAVI=−0.012+0.002×ΔHR, r=−0.07, p=0.56, data not shown).

2. Effect of doxazosin administration on blood pressure, ba PWV and CAVI (Fig. 1B)

When doxazosin (4 mg) was administered to the same 12 men, one week later, mean systolic blood pressure started to decrease gradually at 1 hour from 130.2 ± 4.6 mmHg to 117.2 ± 4.8 mmHg (mean ± SE) at 3 hours (p<0.05), continued to decrease until 4 hours and then began to return, but was still low at 6 hours. Diastolic blood pressure started to decrease at 1 hour from 85.1 ± 4.1 mmHg to 74.2 ± 3.9 mmHg (p

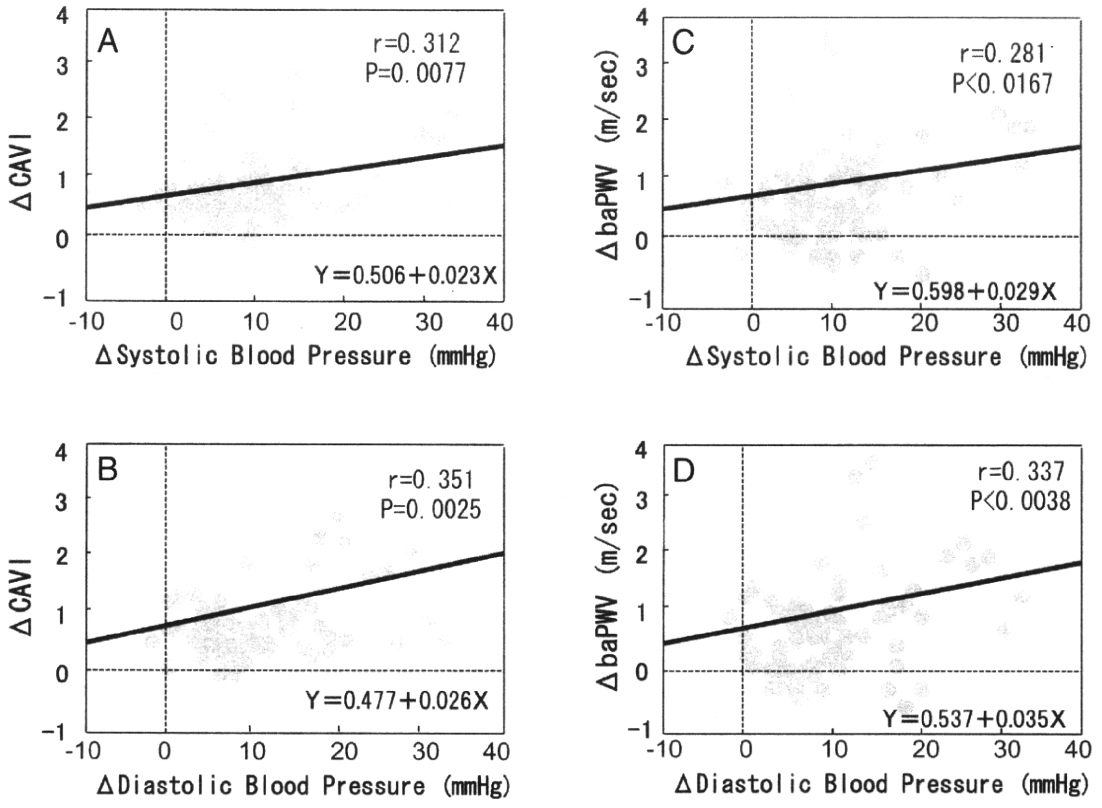

Fig. 3. Correlations between ΔCAVI and ΔbaPWV, and Δblood pressures during doxazosin administration

The differences in vascular parameters (Δ) between before and after doxazosin administration each hour were calculated, and their correlation shown.

A, B: Correlations between ΔCAVI, and Δsystolic pressure (A) and Δdiastolic pressure (B) during doxazosin administration

C, D: Correlations between ΔbaPWV, and Δsystolic pressure (C) and Δdiastolic pressure (D) during doxazosin admnistration

<0.05) at 3 hours, and continued to decrease until 5 hours, and returning slightly at 6 hours.

Heart rate started increase at 1 hour from 71.2 ± 4.4 /min to 79.3 ± 4.6 /min ($p<0.01$) at 3 hours. The increase continued from 3 hours to 6 hours.

baPWV started to decrease at 1 hour from 13.98 ± 0.68 to 12.25 ± 0.53 m/sec at 3 hours significantly ($p<0.05$) and returned from 5 hours.

CAVI also started to decrease at 1 hour from 8.15 ± 0.28 to 7.18 ± 0.37 ($p<0.05$), significantly at 3 hours. This decrease continued at 4 hours and began to return from 5 hours, but was still low at 6 hours, as systolic and diastolic blood pressures decreased.

The differences in vascular parameters (Δ) between before and after doxazosin administration at each hour were calculated, and these correlations are shown in **Fig. 3**. As in **Fig. 3C, D**, ΔbaPWV and Δ systolic blood pressure were significantly correlated (ΔbaPWV = 0.598 + 0.029 × ΔsBP, $r=0.281$, $p=0.0167$). ΔbaPWV and Δdiastolic blood pressure were also significantly correlated (ΔbaPWV = 0.537 + 0.035 × ΔdBP, $r=0.337$, $p=0.0038$).

As in **Fig. 3A, B**, ΔCAVI and Δsystolic blood pressure were significantly correlated (ΔCAVI = 0.506 + 0.023 × ΔsBP, $r=0.31$, $p=0.0077$), and ΔCAVI and Δdiastolic blood pressure were also significantly correlated (ΔCAVI = 0.477 + 0.026 × ΔsBP, $r=0.351$, $p=0.0025$)

ΔbaPWV and Δheart rate were not correlated (ΔbaPWV = 0.911 + 0.001 × ΔHR, $r=0.011$, $p=0.927$, data not shown). ΔCAVI and Δheart rate were negatively correlated (ΔCAVI = 0.628 − 0.024 × ΔHR, $r=0.502$, $p<0.0001$, data not shown).

Discussion

When metoprolol, a β-1 blocker, was administered, systolic and diastolic blood pressure decreased,

and baPWV decreased, but CAVI did not change (**Fig. 1A**). A correlation between ΔbaPWV and Δsystolic and diastolic blood pressure was observed (**Fig. 2C, D**), but correlations between ΔCAVI and Δ systolic and diastolic blood pressures were not observed (**Fig. 2A, B**). These results indicate that baPWV is affected by blood pressure itself at measuring time as Nye pointed out[5], but CAVI was not affected with blood pressure changes induced by decreased heart muscle contraction. Those were comfirmed by no correlations between ΔCAVI and Δsystolic and Δ diastolic blood pressures were found (**Fig. 2A, B**).

When doxazosin was administered, both baPWV and CAVI decreased as systolic and diastolic blood pressures decreased (**Fig. 1B**), and correlations between ΔCAVI and Δsystolic and Δdiastolic blood pressures were observed (**Fig. 3A, B**). CAVI appeared to be decreased by a decrease in blood pressure, but this decrease in CAVI was not directly induced by a decrease in blood pressure, because, as mentioned above, CAVI did not decrease with a decrease in blood pressure by metoprolol. The mechanism by which CAVI decreased during doxazosin administration might be due to doxazosin-induced dilatation of the arterial wall accompaning with a decrease in peripheral vascular resistance.

From these results, it was also suggested that the CAVI value itself was composed of the stiffness of matrix components such as collagen and elastin, proteoglycans[26, 27] and also a contraction of smooth muscle cells[28].

The contraction of vascular smooth muscle cells is under the control of nerves and vasoconstrictive hormones, such as catecholamine[29], angiotensin[30], and also calcium ion[31] as vasoconstrictors, as well as nitric oxide as a vasodilator[32]. The precise those factors influencing CAVI should have to be studied in the future.

The dependency of CAVI on heart rate is another point of discussion. In our study, during doxazosin administration, heart rate increased, but CAVI decreased (**Fig. 1B**), and the Δheart rate and ΔCAVI were negatively correlated; however, during metoprolol administration, the heart rate decreased for 1-2 hours, but CAVI did not change (**Fig. 1A**). It might be suggested that CAVI is independent of the heart rate in the ranges of heart rate from 55-80 beat/min.

The dependency of baPWV on heart rate (90-120 beats/min) has been reported[33], and it could not be denied that baPWV was lowered partly by the decreased heart rate during metoprolol administration rather than blood pressure; however, during doxazosin administration (**Fig. 1B**), the heart rate actually increased, but baPWV decreased. From our study, the relationship between baPWV and heart rate around 60-80 beats/min could not be mentioned.

In summary, our studies suggested that CAVI was independent of blood pressure at the time of measurement, and also suggested that CAVI could be affected by the changes of contratility of arterial smooth muscle cells.

References

1) Asmar R: Pulse wave velocity principles and measurement P25-55, in Arterial stiffness and pulse wave velocity edited by Asmar R, O'Rourke MF, Safar M, Elsevier Amsterdam, 1999
2) Bramwell JC, Hill AV: Velocity of the Pulse wave in Man. Proc. Roy. Soc., 1922; B: 298-306
3) Hallock P: Arterial elasticity in man in relation to age as evaluated by the pulse wave velocity method. Arch. Intern, 1934; 54: 770-798
4) Hamilton, W. F., Remington, J. W., and Dow, P: The determination of the propagation velocity of the arterial pulse wave. Amer. J. Physiol., 1945; 144: 521-535
5) Nye ER: The effect of blood pressure alteration on the pulse wave velocity. Bri. Heart J., 1964; 266: 261-265
6) Blacher J, Asmar R, Djane S, London GM, Safar ME: Aortic pulse wave velocity as a marker of cardiovascular risk in hypertensive patients. Hypertension, 1999 May; 33(5): 1111-1117
7) Yamashina A, Tomiyama H, Takeda K, Tsuda H, Arai T, Koji Y, Hori S, Yamamoto Y: Validity, Reproducibility, and Clinical Significance of Noninvasive Brachial-Ankle Pulse Wave Velocity Measurement. Hypertension Research Hypertens Res, 2002; 25: 359-364
8) Kim HJ, Nam JS, Park JS, Cho M, Kim CS, Ahn CW, Kwon HM, Hong BK, Yoon YW, Cha BS, Kim KR, Lee HC: Usefulness of brachial-ankle pulse wave velocity as a predictive marker of multiple coronary artery occlusive disease in Korean type 2 diabetes patients. Diabetes Res Clin Pract, 2009 Jul; 85(1): 30-34
9) Hasegawa M: Fundamental research on human aortic pulse wave velocity. Jikei Medical Journal, 1970; 85: 742-760
10) Hamazaki T, Urakaze M, Sawazaki S, Yamazaki K, Taki H, Yano S: Comparison of pulse wave velocity of the aorta between inhabitants of fishing and farming villages in Japan. Atherosclerosis, 1988; 73: 157-160
11) Saito Y, Shirai K, Utino J, Okazaki M, Hattori Y,Yoshida T, Yoshida S: Effect of nefedipine administration on pulse wave velocity of chronic hemodialysis patients-2 years trial. Cardiovascular Drug Therapy, 1990; 4: 987-990
12) Shirai K, Utino J, Otsuka K, Takata M: A novel blood pressure-independent arterial wall stiffness parameter; cardio-ankle vascular index (CAVI). J Atheroscler Thromb, 2006; 13(2): 101-107
13) Kubozono T, Miyata M, Ueyama K, Nagaki A, Otsuji Y, Kusano K, Kubozono O, Tei C: Clinical significance and reproducibility of new arterial distensibility index. Circ J,